

# CLAVATA signaling ensures reproductive development in plants across thermal environments

Daniel S. Jones<sup>1</sup>, Amala John<sup>1</sup>, Kylie R. VanDerMolen<sup>1</sup>, and Zachary L. Nimchuk<sup>1,2,3</sup>

<sup>1</sup>Department of Biology, University of North Carolina at Chapel Hill, 250 Bell Tower Dr., Chapel Hill, North Carolina, 27599, USA.

<sup>2</sup>Curriculum in Genetics and Molecular Biology, University of North Carolina at Chapel Hill, Chapel Hill, North Carolina, USA.

### <sup>3</sup>Lead Contact

Correspondence: [zackn@email.unc.edu](mailto:zackn@email.unc.edu)

## SUMMARY

15 The ability to thrive in diverse environments requires that species maintain development and  
16 reproduction despite dynamic conditions. Many developmental processes are stabilized through  
17 robust signaling pathways which cooperatively ensure proper development [1]. During  
18 reproduction, plants like *Arabidopsis thaliana* continuously generate flowers on growing  
19 indeterminate inflorescences [2]. Flower primordia initiation and outgrowth depends on the  
20 hormone auxin and is robust across diverse environments [3-6]. Here we show that reproductive  
21 development under different thermal conditions requires the integration of multiple pathways  
22 regulating auxin dependent flower production. In colder/ambient temperatures, the receptor  
23 complex CLAVATA2/CORYNE (CLV2/CRN) is necessary for continuous flower outgrowth during  
24 inflorescence development. CLV2/CRN signaling is independent of CLAVATA1 (CLV1)-related  
25 receptor signaling but involves the CLAVATA3 INSENSTIVE RECEPTOR KINASE (CIK) family  
26 co-receptors, with higher order *cik* mutant combinations phenocopying *clv2/crn* flower outgrowth  
27 defects. Developing *crn* inflorescences display reduced auxin signaling and restoration of auxin  
28 biosynthesis is sufficient to restore flower outgrowth in colder/ambient temperatures. In contrast,  
29 at higher temperatures both *clv2/crn* signaling and heat induced auxin biosynthesis via YUCCA  
30 family genes are synergistically required to maintain flower development. Our work reveals a

31 novel mechanism integrating peptide hormone and auxin signaling in the regulation of flower  
32 development across diverse thermal environments.

33

34 **RESULTS AND DISCUSSION**

35 Plants continually develop new organs throughout their life and do so across varied environmental  
36 conditions [7]. This indeterminate growth requires balanced cell proliferation and differentiation in  
37 stem cell niches, called meristems, at growing apices [8, 9]. During the reproductive phase of  
38 *Arabidopsis thaliana*, flower primordia are continuously produced from inflorescence meristems  
39 (IM) dependent on the hormone auxin [3-6]. Primordia then proliferate, forming flowers from  
40 secondary floral meristems [10, 11]. Cell recruitment into flower primordia is balanced by  
41 proliferation in the IM center. The conserved CLAVATA3 (CLV3) peptide signaling pathway  
42 dampens stem cell proliferation in shoot and floral meristems [12, 13]. CLV3 signals through a  
43 suite of receptors which repress the expression of *WUSCHEL* (*WUS*) in the center of the IM [8,  
44 14]. *WUS* encodes a homeobox transcription factor that positively regulates stem cell proliferation  
45 [15]. Among these receptors is the atypical receptor pair CLAVATA2/CORYNE (CLV2/CRN), a  
46 leucine rich repeat (LRR) receptor-like protein and a transmembrane pseudokinase, respectively  
47 [16-19]. CLV2/CRN negatively regulate IM stem cell proliferation independent of other CLV3  
48 receptors [17, 20]. Here we define a new role for CLV2/CRN in promoting auxin-dependent flower  
49 primordia outgrowth and show that signaling through this receptor complex contributes to an  
50 environmental buffering mechanism which ensures reproductive developmental stability.

51

52 **The CLV2/CRN receptor complex promotes flower primordia outgrowth and development**

53 After the production of 1-5 normal flowers in *crn* null mutants (*crn-10*; in the Col-0 ecotype), we  
54 noticed a novel phenotype in which flower primordia initiate but fail to develop further and  
55 inflorescence internode elongation stalls (Figures 1A-1B; the termination phase). After ~30-40 of  
56 these terminated primordia, flower development and inflorescence elongation resumes (recovery

57 phase), indicating that continuous flower production requires *CRN* (Figures 1B and S1A; Movie  
58 *S1*). *c/v2* null mutants (*rlp10-1*; in Col-0) displayed a similar phenotype to *crn* (Figure 1C), which  
59 was previously observed in *c/v2* in a survey of mutants in receptor-like protein genes, but not  
60 characterized [21]. To quantify primordia termination, we classified the first 30 attempts to make  
61 flowers along the primary inflorescence as normal (complete flowers; formation of all four flower  
62 organs [22]), terminated flower primordia (no flower organs develop), or terminated flowers (some  
63 flower organs develop, but no gynoecium). *crn* and *c/v2* single mutants displayed equivalent  
64 defects in flower production (Figure 1E), also observed in *c/v2 crn* double mutants, consistent with  
65 the documented co-function of CLV2/CRN (Figures 1B-E). *c/v2/crn* flower outgrowth defects, and  
66 floral meristem size (measured in carpels made per flower), were complemented by expressing  
67 fusion proteins from their native promoters (Figure S1B-S1C and S1I-S1J). Using standardized  
68 flower primordia staging, we found that *crn* primordia outgrowth deviated from WT (wild type) at  
69 flower primordia stage three (FP3), with little proliferation occurring afterwards (Figures 1F-1G;  
70 staging as in [23], or stage 2 using Smyth *et. al.* stages [22]). In *crn*, terminated primordia fail to  
71 develop floral organs, but occasionally produce bract-like structures, likely due to de-repression  
72 of cryptic bract outgrowth (Figure 1H) [24].

73

74 Consistent with a role in flower primordia development, *CRN* expression was detected as early  
75 as incipient primordia (before primordia outgrowth) and remained throughout primordia formation  
76 (Figure 1I). Both *CRN* (*CRN-GFP*) and *CLV2* (*CLV2-Citrine*) fusion proteins, expressed by native  
77 promoters, confirmed this expression pattern (Figures S1B and S1C). Supporting previous *in situ*  
78 results [15], *WUS* expression did not overlap with *CRN* spatially or temporally during primordia  
79 specification and outgrowth, when *crn* inflorescence phenotypes diverge from WT (Figures 1I and  
80 1J). The *WUS* domain was expanded in *crn* IMs compared to WT but ectopic *WUS* expression  
81 was not detected in terminated *crn* primordia (Figures 1J and 1K) [17]. Additionally, other mutants

82 known to have expanded *WUS* IM expression domains do not display *c lv2/crn* primordia  
83 outgrowth defects (see below).

84

85 CLV2/CRN functions have been studied extensively in the Landsberg-*erecta* (Ler) background  
86 [16, 17, 25]. We found no flower primordia outgrowth defects in null *c lv2-1* mutants in Ler,  
87 explaining why this phenotype has not been described in this ecotype (Figures S1D-S1E and S1I-  
88 S1J). Flower primordia termination was also not observed in *crn-1* (Ler background [17]) or two  
89 CRISPR-derived null alleles of *c lv2* in Ler (*c lv2-10* and *c lv2-11*; Figures S1F-S1H and S1I-S1K).  
90 F1 plants from an ecotype-hybrid *c lv2* null cross of *r/p10-1* (Col-0) X *c lv2-1* (Ler) displayed mild  
91 termination (Figure S1L). Flower primordia outgrowth defects segregated in a digenic semi-  
92 dominant manner in the F2 population (Figure S1M), indicating that dominant modifiers in Col-0  
93 underlie ecotype differences in *c lv2/crn* flower outgrowth. Additionally, ecotypic differences were  
94 not attributable to the *erecta* (*er*) allele in Ler plants [26], as *c lv2 er* double mutants in the Col-0  
95 background had equivalent flower outgrowth defects to *c lv2* (Figures S1N-S1P). Double mutants  
96 between *CLV2* and the floral identity gene *LEAFY* (*LFY*; *c lv2 lfy*) displayed primordia outgrowth  
97 defects and *lfy*-like floral organ conversions (Figures S1Q-S1R), indicating that *CLV2/CRN*  
98 promote primordia formation independent of *LFY*-floral meristem specification [10, 27].  
99 Collectively, these data show that *CLV2/CRN* signaling represents a novel ecotype-dependent  
100 process regulating primordia outgrowth following reproductive transition.

101

## 102 **CLAVATA2/CRN-mediated flower outgrowth requires CIK co-receptors**

103 The *CLV2/CRN* receptor complex lacks signaling capacity alone, as *CRN* is a transmembrane  
104 pseudokinase [19], suggesting *CLV2/CRN* require associated functional kinase(s) to signal.  
105 *CLAVATA* candidates with active kinase domains include the *CLAVATA3 INSENSTIVE*  
106 *RECEPTOR KINASE1/2/3/4* (CIK1/2/3/4) family co-receptors, *CLV1* and the *CLV1*-related  
107 *BARELY ANY MERISTEM1/2/3* receptors (BAM1/2/3), which all regulate IM stem cell proliferation

108 [28-31]. CLV1/BAM signals independent of CLV2/CRN in shoot and floral stem cell control [20].  
109 Consistent with this, we found negligible amounts of flower primordia termination in *clv1*, *bam1/2*,  
110 or *bam1/2/3* null mutants (in Col-0) and *crn* was additive in each higher order mutant combination  
111 (*crn clv1*, *crn bam1/2*, and *crn bam1/2/3*; Figures S2A-S2J). CIK1/2/3/4 are leucine-rich repeat  
112 (LRR)-II-receptor-like-kinase subfamily co-receptors with overlapping functions with CLAVATA  
113 primary receptors, several of which physically interact with CRN [31]. In a previous report we  
114 noticed a *crn*-like phenotype in specific *cik* mutant combinations [31]. To confirm this observation,  
115 we generated higher order CRISPR null alleles of *CIK1/2/4* in Col-0 (Figure S2K). In contrast to  
116 *clv1/bam* mutants, *cik1/2/4* displayed flower primordia termination equivalent to *crn* (Figures 2A-  
117 2C). Additionally, *cik1/2/4* had enlarged floral meristems quantitatively similar to *crn* (Figure 2D).  
118 The protein phosphatase POLTERGEIST (POL), a downstream component of CLAVATA  
119 signaling, suppresses *clv2/crn* meristem size defects [17, 32]. *pol* restored flower outgrowth and  
120 internode elongation defects in *crn* (*crn pol*; Figures 2E-2H). Collectively, these data demonstrate  
121 that CLV2/CRN signal alongside CIK1/2/4 co-receptors to promote flower outgrowth through a  
122 POL-dependent pathway.

123

124 CLAVATA receptors respond to CLAVATA3(CLV3)/EMBRYO-SURROUNDING REGION (CLE)  
125 peptide ligand(s), and there are 32 *CLEs* in Arabidopsis [33]. CLV3 and a suite of redundant CLE  
126 peptides signal via CLV1 to repress IM stem cell proliferation parallel to CLV2/CRN [13, 17, 34,  
127 35]. Flower primordia outgrowth is not impaired in *clv3* or *dodeca-cle* higher order mutants, which  
128 combine *clv3* with several redundant *cle* alleles [13], suggesting that additional unknown CLE  
129 peptides regulate flower outgrowth through CLV2/CRN/CIK (Figure S2L-S2M). Consistent with  
130 this, *crn clv3* double mutants are additive with a clear disruption in flower primordia outgrowth and  
131 an enlarged disc-like IM (Figure S2N). The enlarged shoot and fasciated stem of *crn clv3* made  
132 quantification of terminated primordia difficult; however, these data support previous work  
133 suggesting that CLV2/CRN can act independently of CLV3 [20].

134

135 **Temperature and *CLV2/CRN* modulate auxin-dependent flower primordia outgrowth**

136 Many developmental programs are robust, ensuring optimal morphology/function across varied  
137 conditions [13, 36]. Populations of *A. thaliana* can be found throughout the Northern Hemisphere  
138 thriving in diverse environments [7, 37]. Natural variation in traits like flowering time and freezing  
139 tolerance are influenced by and/or directly correlated with adaptations to local conditions [7].  
140 While investigating *clv2/crn* we observed remarkable quantitative variability in flower primordia  
141 termination at different temperatures. Flower outgrowth defects in *clv2/crn* were suppressed when  
142 grown at higher temperatures (31°C) compared to colder/ambient temperatures (16°C/24°C;  
143 Figures 3A-3G). Previous work noted shoot defects in *crn-1* mutants (Ler background) at high  
144 temperatures; however, we did not observe this under our conditions (Figures 3H-3I) [17].  
145 Thermomorphogenic pathways regulate high temperature seedling growth by enhancing auxin  
146 biosynthesis [38, 39]. At higher temperatures, PHYTOCHROME INTERACTING FACTOR (PIF)  
147 family transcriptional regulators activate *YUCCA* (*YUC*) genes, which encode rate-limiting  
148 enzymes in auxin biosynthesis [40, 41]. Under colder/ambient temperatures,  
149 thermomorphogenesis is negatively regulated by the transcriptional repressor EARLY  
150 FLOWERING 3 (ELF3) [42]. As such, *elf3* seedlings display constitutive thermomorphogenic  
151 responses and higher auxin production across temperatures. To test if the thermomorphogenesis  
152 pathway was sufficient to suppress *clv2/crn* flower outgrowth defects, we generated *crn elf3*  
153 double mutants and grew them at colder/ambient temperatures. Consistent with high temperature  
154 mediated suppression of *crn*, flower primordia termination was suppressed in *crn elf3* at colder  
155 temperatures (Figures 3J-3L). In contrast to the suppression of *crn* primordia outgrowth, *elf3*  
156 slightly enhanced carpel numbers compared to *crn* (Figure 3M). This finding supports that  
157 *CLV2/CRN*-mediated outgrowth and *CLV2/CRN*-mediated meristem size regulation are  
158 separable with primordia outgrowth being highly sensitive to thermal conditions. Our data shows  
159 that *CLV2/CRN/CIK* signaling is critical for continuous flower production at colder/ambient

160 temperatures but can be bypassed by thermomorphogenic responses to higher temperatures. As  
161 such, while *Arabidopsis* flower development is robust under various environmental conditions,  
162 distinct mechanisms maintain this stability across different temperatures.

163

164 To define the mechanisms underlying *crn* primordia termination, we used RNA-seq to identify  
165 differentially expressed genes (DEGs) in terminating *crn* IMs compared to WT. Using a strict cutoff  
166 (p-value < 0.001), we found 460 DEGs between *crn* and WT IMs, with 236 upregulated and 224  
167 downregulated in *crn* (Figure 4A; Table S1). Enriched Gene Ontology (GO) terms among DEGs  
168 included meristem maintenance, flower development, and auxin function (Figure 4B; Table S2)  
169 [43-45]. The first two GO term groups are consistent with CRN's role in meristem maintenance  
170 [17, 20], and flower development, documented in this study (Tables S1 and S2). The  
171 overrepresentation of auxin-associated genes in *crn* IM DEGs (Table S1) is complementary to the  
172 thermomorphogenic suppression of *crn*'s primordia termination (Figure 3), suggesting CLV2/CRN  
173 regulate auxin function during early flower primordia outgrowth. Therefore, we asked if *clv2/crn*  
174 were defective in auxin outputs at lower temperatures and if auxin biosynthesis was required for  
175 the high temperature suppression of *clv2/crn*. We visualized the auxin signaling reporter  
176 *DR5::GFP* (where GFP positively correlates with increased auxin signaling output) and the auxin  
177 perception reporter *DII::Venus* (where Venus negatively correlates with increased auxin  
178 perception) in terminating *crn* IMs [46, 47]. There was a significant reduction in *DR5::GFP* signal  
179 in *crn* IMs during termination, specifically in the L1 layer of incipient primordia (Figures 4C-4D and  
180 S3A-S3C). Consistently, *DII::Venus* accumulated in the L1 layer of terminated *crn* IMs, a pattern  
181 never observed in WT (Figures 4E-4F and S3D). *DR5::GFP* was restored to WT levels during  
182 *crn*'s recovery phase (Figures S3E-S3F). During flower development, the PIN-FORMED1 (PIN1)  
183 auxin efflux transporter concentrates auxin to the IM periphery, creating local maxima which  
184 trigger flower primordia initiation and subsequent outgrowth [4, 5]. PIN1 reporter levels (PIN1-  
185 GFP) [5] were decreased in terminating *crn* IMs (Figures S3G-S3H); consistent with *PIN1*

186 expression from our RNAseq DEG data. (Table S1). PIN1-GFP levels increased during *crn*'s  
187 recovery phase, but not to WT levels (Figure S3I). These data demonstrate an overall reduction  
188 in auxin signaling/perception within the IM and developing primordia of *crn* during the termination  
189 phase. This decrease is transient and corresponds with flower outgrowth defects, indicating that  
190 CLV2/CRN positively regulate auxin dependent flower primordia outgrowth in the IM.

191

192 Several auxin biosynthetic genes had decreased expression in *crn* compared to WT, including  
193 *YUC* genes that regulate flower development (Figure S3J and Table S3) [48]. To test if low auxin  
194 levels contributes to *crn*'s flower outgrowth defects, we expressed *YUC1* in developing primordia  
195 of *crn* using the *AINTEGUMENTA* promoter (*ANTp::YUC1*) [6, 49] and grew plants in colder (16-  
196 18°C) and ambient (22-24°C) temperatures. At 22-24°C, 9/13 T1 plants suppressed *crn* while only  
197 2/18 plants partially suppressed *crn* at 16-18°C (Figures 4G-4H). This demonstrates that at  
198 ambient temperatures (where *crn* terminates), ectopic *YUC1* can suppress flower outgrowth  
199 defects; however, the degree of suppression correlates with temperature. Higher order mutant  
200 combinations in IM-expressed *YUC1/2/4/6* severely impair floral and vasculature development;  
201 however, *yuc1/4* double mutants produce more typical inflorescences with identifiable flowers  
202 [48]. We generated *clv2 yuc1/4* triple mutants to reduce YUC-dependent auxin in *clv2* and test  
203 whether high temperature suppression of *clv2/crn* flower termination was dependent on YUC-  
204 mediated auxin biosynthesis. At 16-18°C, *clv2 yuc1/4* triple mutants displayed rates of flower  
205 primordia termination comparable to *clv2* (Figure 4I). As such, CLV2/CRN promote auxin  
206 mediated primordia outgrowth independent of YUC1/4 in colder temperatures. At 28-31°C, some  
207 *clv2 yuc1/4* triple mutant plants displayed *clv2* flower primordia termination, indicating that at high  
208 temperatures YUC1/4 contribute to heat induced suppression (Figure 4J). Surprisingly though,  
209 the majority (~60%) of *clv2 yuc1/4* plants had a synergistic response to high temperatures  
210 resulting in *pin*-like inflorescences completely lacking flower primordia (Figure 4J). These data

211 suggest that high temperature suppression of *c/v2* is dependent on *YUC1/4*-mediated auxin  
212 biosynthesis and that under high temperatures, *CLV2/CRN* and *YUC1/4* are synergistically  
213 required to maintain flower primordia initiation and outgrowth.

214

215 Ensuring robust development and reproduction across environments is a challenge all organisms  
216 face. Here we demonstrate that robust flower production in diverse thermal environments is  
217 achieved through the synergistic deployment of *CLV2/CRN*-signaling and *ELF3*-regulated auxin  
218 production via the thermomorphogenesis pathway in *Arabidopsis*. The relative contribution of  
219 each to flower development varies across thermal clines, with *CLV2/CRN* signaling being critical  
220 at colder/ambient temperatures and synergistic with heat-induced auxin production at higher  
221 temperatures (Figure S4). *Arabidopsis* seedlings respond to high temperatures by promoting  
222 auxin-dependent hypocotyl elongation, a process negatively regulated by *ELF3* [38, 42]. Our work  
223 demonstrates that high temperatures and *ELF3* also regulate auxin-dependent primordia  
224 production. Interestingly, *c/v2 yuc1/4* primordia outgrowth defects were strongly enhanced in  
225 warmer conditions. Higher temperatures also enhance penetrance of seedling defects in loss-of-  
226 function mutants in the TRANSPORT INHIBITOR RESPONSE1 (TIR)-family auxin receptors [50].  
227 As such, heat might have an unappreciated negative impact on auxin function, with  
228 thermomorphogenesis-induced auxin playing a protective role rather than simply directing growth.  
229 How *CLV2/CRN* stimulate auxin-dependent flower initiation is unknown. Ectopic *YUC1*  
230 expression or heat-induced auxin production is sufficient to restore primordia outgrowth to  
231 *c/v2/crn*. This suggests that *CLV2/CRN* are not critically required for TIR-dependent auxin  
232 perception, ARF5/MONOPEROS dependent transcriptional activity, or the TRYPTOPHAN  
233 AMINOTRANSFERASE OF ARABIDOPSIS (TAA1)-mediated conversion of tryptophan to indole-  
234 3-pyruvate (IPA) step upstream of *YUCCA* in auxin biosynthesis [6, 51-53].

235

236 *clv2/crn* defects manifest early in inflorescence development and are transient. Recovery of  
237 primordia production is not linked to flower meristem identity or seed/fruit derived auxin production  
238 (*clv2 lfy* plants). This suggests that the transition from vegetative to reproductive meristem fate  
239 may be sensitized to CLV2/CRN signaling. Nevertheless, *clv2 yuc1/4* plants reveals that  
240 CLV2/CRN signaling is required at later steps in inflorescence development as well. Heat stress  
241 is known to damage crops in ways that negatively impact yield, including the loss of flower  
242 production [54, 55]. As climate change increases global temperatures it will be necessary to  
243 mitigate heat impacts on crop yield. If the environmental buffering capacity of CLV2/CRN-  
244 signaling is conserved in crop species perhaps it could be deployed to help improve plant  
245 responses to climate change.

246

#### 247 **ACKNOWLEDGEMNTS**

248 We thank Yunde Zhao, the ABRC stock center, Paul Tarr, Joe Kieber, and Elena Shpak for  
249 sharing seeds, vectors, and reporter lines. We thank Tony D. Perdue, director of the UNC Biology  
250 Microscopy Core, for assistance with imaging. We thank Jamie Winshell and James Garzoni for  
251 lab and plant growth facility support. We thank UNC's High-Throughput Sequencing Facility for  
252 sequencing services. We thank members of the Nimchuk lab for critical feedback on this project.  
253 This research was supported by a NIGMS-MIRA award from National Institutes of Health  
254 (R35GM119614) and the National Science Foundation (NSF) Plant Genome Research Program  
255 (PGRP; IOS-1546837) to Z.L.N. D.S.J. is supported by an NSF Postdoctoral Research Fellowship  
256 in Biology through the PGRP (NSF# 1906389).

257

#### 258 **AUTHOR CONTRIBUTIONS**

259 D.S.J. designed/Performed experiments, analyzed data, acquired funding for support, and wrote  
260 the manuscript. A.J. designed/Performed experiments and analyzed data. K.R.V performed Col-

261 0 x Ler population experiments. Z.L.N. conceptualized the project and experiments, analyzed  
262 data, acquired funding, and wrote the manuscript.

263

## 264 **DECLARATION OF INTERESTS**

265 The authors declare no competing interests.

266

## 267 **MAIN TEXT FIGURE LEGENDS**

### 268 **Figure 1. Flower primordia outgrowth is disrupted in *clv2/crn***

269 (A-D) Inflorescences of Col-0, *crn* (*crn-10*), *clv2* (*rlp10-1*), and *crn clv2* double mutants. (A'-D')  
270 Close up showing flower primordia termination in *crn*, *clv2* and *crn clv2*.  
271 (E) Quantification of flower termination, classifying the first 30 attempts to make a flower as:  
272 normal (grey), terminated primordia (blue) or terminated flowers (yellow) in Col-0 (n=28), *crn*  
273 (n=27), *clv2* (n=25), and *crn clv2* (n=25).

274 (F and G) 3-D reconstruction of inflorescence meristems of (F) Col-0 (n=4) and (G) *crn* (n=6).  
275 Axial view of the (F', G') third (FP3) and (F'', G'') fourth (FP4) flower primordia (labeled 3 and 4 in  
276 (F) and (G)) revealing developmental differences. FP3 and FP4 were determined by identifying  
277 the 3<sup>rd</sup> and 4<sup>th</sup> earliest detectable primordia along the IM, respectively. Staging similar to [23].

278 (H) Side view of a young inflorescence meristem of *crn* during the termination phase (n=5).

279 (I-K) Expression patterns of *YPET-N7* reporter lines in the IM with XY view of L5 layer (I-K) and  
280 axial view (Z-axis) of same IM stack (I'-K') shown for each: (I) *CRNpro* in Col-0 (n=6), (J) *WUSpro*  
281 in Col-0 (n=6), (K) *WUSpro* in *crn* (n=6). Tissue stained with propidium iodide (PI; magenta).

282 Statistical groupings based on significant differences found using Kruskal-Wallis and Dunn's  
283 multiple comparison test correction (E). Scale bars, 50µm in (H), 20µm in (F-G) and (I-K).

284 See also Figure S1.

285

286 **Figure 2. CLV2/CRN-mediated flower outgrowth requires CIK1/2/4 co-receptors and a**  
287 **downstream *POL*-dependent pathway**

288 (A-B) Inflorescence of *crn* and *cik1/2/4* mutant plants reveal similar flower termination defects.

289 Quantification of (C) flower termination and (D) carpel number across Col-0 (n=16), *crn* (n=17),

290 and *cik1/2/4* (n=13).

291 (E-F) Inflorescence of *crn* and *crn pol* showing that flower termination is suppressed by *pol* (*pol*-

292 6). Quantification of (G) flower termination and (H) carpel number across Col-0 (n=15), *crn* (n=15),

293 *pol* (n=15), and *crn pol* (n=14).

294 Box and whisker plots show full range of data (min to max) with mean marked as “+”.

295 Statistical groupings based on significant differences found using Kruskal-Wallis and Dunn's

296 multiple comparison test correction (C-D and G-H).

297 See also Figure S2.

298

299 **Figure 3. High temperature responses modulate *clv2/crn* flower primordia outgrowth**

300 (A-F) Temperature-dependent inflorescence phenotypes of *crn* compared to Col-0. Flower

301 primordia termination in *crn* is prevalent at (D) 16°C and (E) 24°C, but is suppressed at (F) 31°C.

302 (G) Quantification of flower primordia termination at 16°C: Col-0 (n=8), *crn* (n=9), *clv2* (n=9), *crn*

303 *clv2* (n=7), 24°C: Col-0 (n=9), *crn* (n=9), *clv2* (n=9), *crn clv2* (n=9), and 31°C: Col-0 (n=8), *crn*

304 (n=9), *clv2* (n=9), *crn clv2* (n=6).

305 (H-I) Inflorescences of Ler and *crn-1* grown at 31°C.

306 (J-K) Inflorescences of *elf3* (*elf3-1*) and *crn elf3* grown at 16-18°C

307 (L-M) Quantification of (L) flower primordia termination and (M) carpel number in Col-0 (n=24),

308 *crn* (n=18), *elf3* (n=27), *crn elf3* (n=26) grown at 16-18°C.

309 Box and whisker plots show full range of data (min to max) with mean marked as “+”.

310 Statistical groupings based on significant differences found using Kruskal-Wallis and Dunn's

311 multiple comparison test correction (L-M).

312

313 **Figure 4. Flower primordia outgrowth is maintained by separable auxin-dependent**  
314 **processes in different thermal conditions**

315 (A) Differentially expressed genes (DEG, p-value < 0.001) between *crn* and WT IMs; upregulated  
316 genes (red), downregulated genes (blue).

317 (B) Top GO terms enriched in *crn* DEGs, highlighting terms associated with flower development  
318 (blue), meristem maintenance (green) and auxin (red).

319 (C-D) Maximum intensity projection (MIP) of *DR5::GFP* (teal) in the IM of (C) Col-0 (n=14) and  
320 (D) *crn* (n=12). Stained with PI (magenta). Arrows point to primordia used for DR5  
321 quantification/comparison.

322 (E-F) Axial view showing DII-Venus (green) expression pattern in (E) Col-0 (n=6) and (F) *crn* (n=8)  
323 IMs. Stained with PI (magenta). (E'-F') L1 layer of IMs from (E') Col-0 and (F') *crn* used to quantify  
324 percent of L1 cells with DII marker. Arrows point to organ boundaries where DII reporter can be  
325 detected in the L1 of Col-0 and *crn*.

326 (G-H) Flower primordia termination across independent T1 lines of *ANTpro::YUC1* in *crn*  
327 compared to Col-0 and *crn* when grown at (G) 16-18°C or (H) 22-24°C.

328 (I) *clv2 yuc1/4* inflorescence grown at colder temperatures (16-18°C) and quantification of flower  
329 outgrowth defects in Col-0 (n=9), *clv2* (n=9), *yuc1/4* (n=8), *clv2 yuc1/4* (n=10).

330 (J) *clv2 yuc1/4* pin-like inflorescence grown at hot temperatures (28-31°C) and quantification of  
331 flower outgrowth defects, including instances of pins (pink bar; right y-axis) in Col-0 (n=29), *clv2*  
332 (n=20), *yuc1/4* (n=20), *clv2 yuc1/4* (n=12).

333 Scale bars, 20µm in (C-D) and (E-F), 1mm in (I-J).

334 Bar plots show mean with SEM.

335 See also Figure S3, Tables S1-S3.

336

337 **STAR METHODS**

338 **RESOURCE AVAILABILITY**

339 **Lead Contact**

340 Information and resource/reagent requests should be directed to and will be fulfilled by the Lead

341 Contact, Zachary Nimchuk ([zackn@email.unc.edu](mailto:zackn@email.unc.edu)).

342

343 **Materials Availability**

344 Plasmids and *Arabidopsis* lines made during this study are freely available to academic

345 researchers through the Lead Contact.

346

347 **Data and Code Availability**

348 Raw RNAseq data described in this study has been deposited into the NCBI Short Read Archive

349 (SRA) database under the BioProject PRJNA661065. Code used to analyze gene expression

350 data can be found on the Nimchuk Lab GitHub page (<https://github.com/NimchukLab>). All other

351 source data obtained throughout the course of this work have not been deposited to any public

352 repository but are available upon request from the Lead Contact.

353

354 **EXPERIMENTAL MODEL AND SUBJECT DETAILS**

355 *Arabidopsis thaliana* accession Columbia (Col-0) was used as our primary model system

356 throughout this work. Some phenotypic comparisons were also made with the accession

357 *Landsberg-erecta* (Ler), as noted.

358

359 **Plant growth conditions**

360 Seeds were sterilized and plated on half-strength MS (Murashige-Skoog) media buffered with

361 MES, pH 5.7. Plates were stratified in the dark at 4°C for 2 days and then moved to constant light

362 in a custom-built grow room with environmental control (temperature maintained between 21-

363 25°C), or in a Percival growth chamber (AR-75L3) when growing at a specified temperature. After

364 7-10 days, seedlings were transplanted to soil (Metro-Mix 360/sand/perlite supplemented with  
365 Marathon pesticide and Peter's 20:20:20 [N:P:K] at recommended levels) and then placed back  
366 into the chamber they were germinated in and grown until flowering for phenotypic analysis.

367

## 368 **METHOD DETAILS**

### 369 **Plant materials**

370 Mutant alleles used in this study are all in the Col-0 background, unless otherwise noted, and  
371 information for each is as follows: *crn* (*crn-10*) [20], *crn-1* in Ler [17], *clv2* in Col-0 (*rlp10-1*) [21],  
372 *clv2-1* in Ler [16], *erecta* (*er-105*) [56], *Ify* (*Ify-1*; ABRC CS6228) [27], *clv1* (*clv1-101*) [57], *bam1*  
373 (*bam1-4*) [30], *bam2* (*bam2-4*) [30], *bam3* (*bam3-2*) [30], *pol* (*pol-6*) [58], *clv3* (*clv3-9*) [30],  
374 *dodeca-cle* (*clv3-9*; CRISPR alleles of: *cle9*, *cle10*, *cle11*, *cle12*, *cle13*, *cle18*, *cle19*, *cle20*, *cle21*,  
375 *cle22*, *cle45*) [13], *elf3* (*elf3-1*; ABRC CS3787) [59], *yuc1* (SALK\_106293) [48], and *yuc4*  
376 (SM\_3\_16128) [48]. Information for previously published transgenic complementation and  
377 reporter lines used are as follows: *CRNpro::CRN-GFP* in *crn* [20], *CLV2pro::CLV2-CITRINE* in  
378 *clv2* [60], *WUSpro::Ypet-N7* in Col-0 (gift from Paul Tarr – Caltech), *DR5pro::GFP* in Col-0 [61,  
379 62], *DII-Venus* in Col-0 [63], *PIN1pro::PIN1-GFP* in Col-0 [64]. The *DR5pro::GFP*, *DII-Venus*, and  
380 *PIN1pro::PIN1-GFP* lines were all crossed into *crn* (*crn-10*) for analysis of auxin signaling levels  
381 in *crn* shoots compared to WT.

382

### 383 **CRISPR mutagenesis of *CIK1/2/4* and *CLV2***

384 The *pCUT* vector system was used to simultaneously create *cik1*, *cik2* and *cik4* mutations in the  
385 Col-0 background, making the *cik1/2/4* higher order mutant [65]. Similarly, the *pCUT* system was  
386 used to make multiple unique mutations in *clv2* in the Ler background. A *pENTR-D/TOPO* entry  
387 vector was modified for golden gate cloning by TOPO cloning in *Pmel* and *Bsal* cut sites (*pENTR-*  
388 *GG*). *pENTR-GG* was used to clone tandem cassettes (*cik1/2/4*) or a single cassette (*clv2*) of the

389 U6 promoter, 20 bp guide sequence, and the gRNA scaffold. These guide constructs were then  
390 gateway cloned into *pCUT4GTW* vector that expresses Cas9 from the *UBIQUITIN10* promoter.  
391 Hygromycin resistant plants were selected in the T1 generation and sequenced to detect editing  
392 of the target genes; *CIK1* (AT1G60800), *CIK2* (AT2G23950), and *CIK4* (AT5G45780) or *CLV2*  
393 (AT1G65380). To make stable *cik1/2/4*, T2 seed from editing *cik1/2/4* lines were grown for 2  
394 weeks under standard conditions, heat shocked for 12-24 hours at 35°C [66], and screened for  
395 stable edits using dCAPS primers designed by the indCAPS webtool  
396 (<http://indcaps.kieber.cloudapps.unc.edu/>) [67]. Cas9 was segregated out of plants that had  
397 stable homozygous mutations in *CIK1/2/4*. To make stable *clv2* alleles in Ler, T2 seed, collected  
398 from single branches of T1 plants that had the *clv2* carpel phenotype, were grown in a Percival  
399 growth chamber at 16°C (see above), screened for stable mutations while segregating Cas9 out  
400 prior to phenotypic analysis.

401

#### 402 **Columbia-0 X Landsberg-erecta hybrid *clv2* population**

403 Null *clv2* lines in the Col-0 (*rlp10-1*) and Ler (*clv2-1*) backgrounds were crossed to generate a  
404 hybrid population with fixed *clv2* mutations. Segregation of flower termination traits was assessed  
405 in the F2 generation. Phenotypic ratios were compared to expected values of a single causative  
406 locus (1:2:1) and digenic semi-dominant modifiers (7:6:3) using Chi-squared analysis (Microsoft  
407 Excel v.16.40) to determine the underlying genetic complexity of the ecotypic variability of *clv2*  
408 termination.

409

#### 410 **Generation of binary vectors and transgenic lines**

411 New transgenic lines were generated using floral-dip transformation of binary vectors into  
412 specified backgrounds [68]. *pWUSpro::Ypet-N7* (gift from Paul Tarr – Caltech; cloning methods  
413 as in [69] but with *Ypet-N7*) was transformed directly into *crn* and the transgene was selected on

414 ½ MS plates with Kanamycin. Four independent lines were selected for downstream analysis with  
415 the *WUS* expression domain being equivalent across all lines imaged (see imaging methods for  
416 data acquisition details). For *pCRNpro::Ypet-N7*, a pENTR-D *Ypet-N7* (2xYpet-N7 fusion) entry  
417 vector was recombined by LR reaction into the *pCRNpro::Gateway* binary vector in the *pMOA33*  
418 background [20]. For *pANTpro::YUC1*, the 4 kb 5' *ANT* promoter was amplified from genomic  
419 DNA, and cloned up stream of a gateway::OCS terminator cassette in the *pCR2.1* shuttle vector,  
420 and sequence verified. The resulting *ANTpro::Gateway::OCS* cassette was then mobilized as a  
421 Not1 fragment in to the *pMOA33* binary vector backbone as previously described to create  
422 *pANTpro::GTW*[30]. The *YUC1* CDS was amplified from Arabidopsis Col-0 cDNA and cloned into  
423 the *pENTR-D* topo vector and sequence verified. This vector was then recombined in an LR  
424 reaction into *pANTpro::GTW* to create the *pANTpro::YUC1*.

425

#### 426 **Photography and time-lapse imaging**

427 Unless specified differently below, young inflorescences were staged at similar developmental  
428 timepoints and photographed using a Canon EOS Rebel T5 equipped with a Tokina 100mm f/2.8  
429 AT-X M100 AF Pro D macro lens. Images were edited for brightness and contrast using Gimp  
430 v2.10.4 (<https://www.gimp.org/>). Young inflorescences from Col-0, *crn*, *clv2*, *crn clv2*, *cik1/2/4*,  
431 *yuc1/4*, and *clv2 yuc1/4* (Figures 1A'-D', 2B, 4E-F, and 4H-I) were imaged using a Zeiss Stemi  
432 2000-C stereo microscope equipped with a Zeiss Axiocam 105-color digital camera and acquired  
433 using Zeiss ZEN software. Time-lapse imaging was done using the Lapse-it  
434 (<http://www.lapseit.com/>) app on an iPhone 6 operating iOS 12.3.1. Imaging began with ~3-week-  
435 old Col-0 (WT) and *crn* plants growing in our custom-built grow room. A single image was taken  
436 every 30 minutes over the course of 10-12 days. The final movie was compiled at 30 frames per  
437 sec and exported into iMovie where it was cropped to show only two plants for comparison of  
438 early flowering phenotypes.

439

440 **Confocal microscopy**

441 Live imaging of inflorescence meristems (IMs) was performed as previously reported [20, 70]. We  
442 used either an inverted Zeiss 710 (for: propidium iodide (PI) stained Col-0, *crn*, *CRNpro:Ypet-N7*,  
443 *WUSpro::Ypet-N7*, *DR5pro::GFP*, *DII-Venus*, and *PIN1pro::PIN1-GFP*) or a Zeiss 880 (for  
444 *CRNpro::CRN-GFP* and *CLV2pro::CLV2-CITRINE*) confocal laser scanning microscope  
445 equipped with an inverter (setup described in [71]). Young IMs were dissected immediately  
446 following floral transition in order to analyze expression patterns and reporter levels at the same  
447 developmental stage as *clv2/crn* flower primordia termination. When analyzing reporter status in  
448 recovered IMs of *crn*, shoots were dissected at a later timepoint after flower buds were visibly  
449 developing again. All IMs were briefly (~5 mins for WT and ~15 mins for *crn*) stained with PI (final  
450 concentration of 50 $\mu$ g/mL for WT shoots and 150 $\mu$ g/mL for *crn*) on ice and placed into a petri dish  
451 with 2% agarose (w/v) and immersed in cold water, ensuring no bubbles formed around the IM  
452 [70]. IMs were imaged using a W Plan-APOCHROMAT 40X (NA = 1.0) water dipping objective.  
453 Laser excitation and detected emission ranges were as follows: PI only – laser 561nm diode, PI  
454 channel 600-750nm; Ypet/Venus markers with PI – 514nm argon laser, Ypet channel 520-581nm,  
455 PI channel 655-758nm; GFP markers (on Zeiss 710) with PI – 488nm argon laser, GFP channel  
456 493-556nm, PI channel 598-642nm; GFP on Zeiss 880 with PI – 488nm argon laser, GFP channel  
457 (GaAsP detector) 490-550nm, PI channel (GaAsP detector) 565-610nm; Citrine on Zeiss 880 with  
458 PI – 514nm argon laser, Citrine channel (GaAsP detector) 519-550nm, PI channel (GaAsP  
459 detector) 565-610nm. Whole IMs were imaged as a z-stack series with a step size optimized for  
460 three-dimensional reconstruction of data. All images comparing reporter levels in different  
461 backgrounds were obtained with identical specifications: *DR5pro::GFP*, *DII-Venus*, and  
462 *PIN1pro::PIN1-GFP* in both WT and *crn* shoots. Live inflorescence micrographs were all post-  
463 processed using ZEN (Zeiss) for three-dimensional reconstructions of IMs and Fiji/ImageJ v.2.0.0-  
464 rc-69/1.52u (National Institutes of Health) [72] for single scan images as well as axial views of

465 IMs. Channels corresponding to PI staining in *crn* IMs were almost always gamma corrected (0.8)  
466 as penetrance of this fluorescent dye in enlarged *crn* shoots was sometimes limited. *DR5pro::GFP*  
467 fluorescence quantification comparing WT and *crn* IMs was done as follows using Fiji/ImageJ  
468 v.2.0.0-rc-69/1.52u. Z-stacks were rendered as maximum intensity projections of the GFP  
469 channel only using data from the entire IM. A region of interest (ROI) was drawn around each of  
470 the first 3 developing primordia (identified as the 3 early primordia with the highest GFP  
471 intensities). GFP levels were quantified for each ROI, normalized to the final area of each ROI,  
472 and then averaged together to obtain a single value for WT and *crn* IMs. DII-Venus quantification  
473 was done using Fiji/ImageJ v.2.0.0-rc-69/1.52u. Due to rapid photobleaching of the Venus  
474 fluorescent reporter, single scan images were taken in the L1 layer of WT and *crn* IMs prior to z-  
475 stack scans and used for direct comparison. The percentage of L1 cells with the Venus reporter  
476 were determined across all imaged IMs, with WT IMs never having reporter in this layer.

477

478 Whole shoot reconstruction of *crn* during termination (Figure 1H) was done using fixed and  
479 cleared tissue, imaging structural autofluorescence (as in [13]). Young *crn* IM were fixed in FAA  
480 (2% formaldehyde, 5% acetic acid, 60% ethanol (w/v)) at 4°C overnight and then dehydrated in a  
481 graded ethanol series (70%, 80%, 95% and 100%) for 30 minutes each at room temperature.  
482 Tissue was then cleared overnight in methyl salicylate (catalog no. M6752; Sigma Aldrich) and  
483 placed in a small glass-bottom petri dish (catalog no. P35G-1.5-10-C; MatTek Corporation) and  
484 imaged on a Zeiss 710 CLSM using a Plan-APOCHROMAT 10X (NA = 0.45). Autofluorescence  
485 was detected using a 488nm argon laser for excitation and combining two channels for emission  
486 detection; Channel 1 – 504-597nm and channel 2 – 629-731nm. Data was gathered as a z-stack  
487 and three-dimensional reconstruction was done in Nikon NIS-Elements as a shaded render of  
488 both channels combined in grayscale.

489

490 **RNA Sequencing and Data Analysis**

491 Total RNA was isolated using the EZNA Plant RNA kit (Omega Bio-tek) from 45-50 inflorescence  
492 meristems for three biological replicates of both Col-0 and *crn* (*crn-10*) plants. RNA was treated  
493 with RNase-free DNase (Omega Bio-tek). Approximately 1.5 ug RNA was used as input material  
494 for library preparation, using the Stranded mRNA-Seq kit (Kapa Biosystems) at the High-  
495 throughput Sequencing Facility at UNC Chapel hill. 50bp paired-end reads were generated on  
496 the NovaSeq 6000 sequencer (illumina) with a read depth of 23-35 million reads per biological  
497 replicate. Trimmed raw data was aligned to the *A. thaliana* genome (TAIR10.1) using HISAT2  
498 version 2.2.0 [73] and reads were counted using Subread version 1.5.1 [74]. Subsequent analysis  
499 was performed on RStudio with reads normalized using EDASeq version 2.22.0 [75] and RUVseq  
500 version 1.22.0 (upper quartile normalization) [76] and differentially expressed genes were  
501 identified with a p-value <0.001 using EdgeR version 3.33.0 [77]. These top 460 DEGs were used  
502 for GO term analysis from Panther [78]. To obtain the average TPM counts of auxin biosynthetic  
503 genes, reads were pseudoaligned to the *Arabidopsis* transcriptome (TAIR10 from  
504 plants.ensembl.org) using Kallisto version 0.44.0 [79] and quantified with Sleuth version 0.33.0  
505 [80].

506

507 **QUANTIFICATION AND STATISTICAL ANALYSIS**

508 Quantitative data from all experiments was compiled and analyzed in GraphPad Prism v.8.3.2.  
509 We performed at least two biological replicates for each experiment ensuring consistent results  
510 (sample sizes indicated in figure legends). For comparisons of flower termination across  
511 conditions, genotypes and/or transgenic lines (Figures 1E, 2C, 2G, 3G, 3L, 4G-H, S1I, S2C-D,  
512 S2I-J), only % flower primordia termination (as defined in the paper) was compare across samples  
513 using a non-parametric Kruskal-Wallis and a Dunn's multiple comparison test correction where  
514 significance was defined as p-value < 0.05. For comparisons of carpel number across genotypes  
515 (Figures 2D, 2H, 3M, and S1J), 10 consecutive flowers on the primary inflorescence were

516 counted, starting after the recovery phase in *crn*, *clv2*, and *cik1/2/4* while starting at the 11<sup>th</sup> flower  
517 in genotypes that had no flower primordia termination or partially suppressed flower primordia  
518 termination (Col-0, Ler, *clv2-1*, *crn-1*, *pol*, *crn pol*, *elf3*, and *crn elf3*). Carpel number was  
519 compared statistically using a non-parametric Kruskal-Wallis and a Dunn's multiple comparison  
520 test correction where significance was defined as p-value < 0.05. For comparison of *DR5pro::GFP*  
521 levels, WT and *crn* IM values were compared statistically using an unpaired t-test, where the p-  
522 value = 0.0007. Sample size (n) for all analyses can be found with each figure in the legend and  
523 refers to the number of individual plants analyzed.

524

## 525 **SUPPLEMENTAL INFORMATION**

526 **Table S1. Normalized differentially expressed genes (DEG) list in *crn* IMs. Related to Figure**  
527 **4 and Table S2**

528 Genes with p-value < 0.001 showing their log2FC, p-value and false discovery rate (FDR). Red  
529 log2FC values indicate upregulation and blue log2FC values indicate downregulation. Red, green  
530 and blue highlights refer to GO processes indicating auxin, meristem and floral related genes,  
531 respectively, while purple highlights indicate the gene belongs to multiple of these groups.

532

## 533 **Movie S1 – Time-lapse of flower termination and recovery in *crn*. Related to Figure 1**

534 Time-lapse of Col-0 (left) and *crn* (right) during early stages of flowering revealing both *crn*'s  
535 termination and recovery phases. Entire movie spans ~10 days. Movie rendered at 30 frames per  
536 second while each frame was captured in 30-minute intervals (see methods).

537

## 538 **References**

539 1. Hallgrímsson, B., Green, R.M., Katz, D.C., Fish, J.L., Bernier, F.P., Roseman, C.C.,  
540 Young, N.M., Cheverud, J.M., and Marcucio, R.S. (2019). The developmental-genetics of

- 541 canalization. In *Seminars in cell & developmental biology*, Volume 88. (Elsevier), pp. 67-  
542 79.
- 543 2. Bradley, D., Ratcliffe, O., Vincent, C., Carpenter, R., and Coen, E. (1997). Inflorescence  
544 commitment and architecture in *Arabidopsis*. *Science* **275**, 80-83.
- 545 3. Reinhardt, D., Mandel, T., and Kuhlemeier, C. (2000). Auxin regulates the initiation and  
546 radial position of plant lateral organs. *The Plant Cell* **12**, 507-518.
- 547 4. Benková, E., Michniewicz, M., Sauer, M., Teichmann, T., Seifertová, D., Jürgens, G., and  
548 Friml, J. (2003). Local, efflux-dependent auxin gradients as a common module for plant  
549 organ formation. *Cell* **115**, 591-602.
- 550 5. Heisler, M.G., Ohno, C., Das, P., Sieber, P., Reddy, G.V., Long, J.A., and Meyerowitz,  
551 E.M. (2005). Patterns of auxin transport and gene expression during primordium  
552 development revealed by live imaging of the *Arabidopsis* inflorescence meristem. *Current  
553 biology* **15**, 1899-1911.
- 554 6. Yamaguchi, N., Wu, M.-F., Winter, C.M., Berns, M.C., Nole-Wilson, S., Yamaguchi, A.,  
555 Coupland, G., Krizek, B.A., and Wagner, D. (2013). A molecular framework for auxin-  
556 mediated initiation of flower primordia. *Developmental cell* **24**, 271-282.
- 557 7. Weigel, D. (2012). Natural variation in *Arabidopsis*: from molecular genetics to ecological  
558 genomics. *Plant physiology* **158**, 2-22.
- 559 8. Somssich, M., Je, B.I., Simon, R., and Jackson, D. (2016). CLAVATA-WUSCHEL  
560 signaling in the shoot meristem. *Development* **143**, 3238-3248.
- 561 9. Pierre-Jerome, E., Drapek, C., and Benfey, P.N. (2018). Regulation of division and  
562 differentiation of plant stem cells. *Annual review of cell and developmental biology* **34**,  
563 289-310.
- 564 10. Weigel, D., Alvarez, J., Smyth, D.R., Yanofsky, M.F., and Meyerowitz, E.M. (1992). LEAFY  
565 controls floral meristem identity in *Arabidopsis*. *Cell* **69**, 843-859.

- 566 11. Pidkowich, M.S., Klenz, J.E., and Haughn, G.W. (1999). The making of a flower: control  
567 of floral meristem identity in *Arabidopsis*. *Trends in plant science* 4, 64-70.
- 568 12. Clark, S.E., Running, M.P., and Meyerowitz, E.M. (1995). CLAVATA3 is a specific  
569 regulator of shoot and floral meristem development affecting the same processes as  
570 CLAVATA1. *Development* 121, 2057-2067.
- 571 13. Rodriguez-Leal, D., Xu, C., Kwon, C.-T., Soyars, C., Demesa-Arevalo, E., Man, J., Liu, L.,  
572 Lemmon, Z.H., Jones, D.S., and Van Eck, J. (2019). Evolution of buffering in a genetic  
573 circuit controlling plant stem cell proliferation. *Nature genetics* 51, 786-792.
- 574 14. Soyars, C.L., James, S.R., and Nimchuk, Z.L. (2016). Ready, aim, shoot: stem cell  
575 regulation of the shoot apical meristem. *Current opinion in plant biology* 29, 163-168.
- 576 15. Mayer, K.F., Schoof, H., Haecker, A., Lenhard, M., Jürgens, G., and Laux, T. (1998). Role  
577 of WUSCHEL in regulating stem cell fate in the *Arabidopsis* shoot meristem. *Cell* 95, 805-  
578 815.
- 579 16. Jeong, S., Trotochaud, A.E., and Clark, S.E. (1999). The *Arabidopsis* CLAVATA2 gene  
580 encodes a receptor-like protein required for the stability of the CLAVATA1 receptor-like  
581 kinase. *The Plant Cell* 11, 1925-1933.
- 582 17. Müller, R., Bleckmann, A., and Simon, R. (2008). The receptor kinase CORYNE of  
583 *Arabidopsis* transmits the stem cell-limiting signal CLAVATA3 independently of  
584 CLAVATA1. *The Plant Cell* 20, 934-946.
- 585 18. Bleckmann, A., Weidtkamp-Peters, S., Seidel, C.A., and Simon, R. (2010). Stem cell  
586 signaling in *Arabidopsis* requires CRN to localize CLV2 to the plasma membrane. *Plant  
587 physiology* 152, 166-176.
- 588 19. Nimchuk, Z.L., Tarr, P.T., and Meyerowitz, E.M. (2011). An evolutionarily conserved  
589 pseudokinase mediates stem cell production in plants. *The Plant Cell* 23, 851-854.
- 590 20. Nimchuk, Z.L. (2017). CLAVATA1 controls distinct signaling outputs that buffer shoot stem  
591 cell proliferation through a two-step transcriptional compensation loop. *PLoS genetics* 13.

- 592 21. Wang, G., Ellendorff, U., Kemp, B., Mansfield, J.W., Forsyth, A., Mitchell, K., Bastas, K.,  
593 Liu, C.-M., Woods-Tör, A., and Zipfel, C. (2008). A genome-wide functional investigation  
594 into the roles of receptor-like proteins in *Arabidopsis*. *Plant physiology* 147, 503-517.
- 595 22. Smyth, D.R., Bowman, J.L., and Meyerowitz, E.M. (1990). Early flower development in  
596 *Arabidopsis*. *The Plant Cell* 2, 755-767.
- 597 23. Reddy, G.V., Heisler, M.G., Ehrhardt, D.W., and Meyerowitz, E.M. (2004). Real-time  
598 lineage analysis reveals oriented cell divisions associated with morphogenesis at the  
599 shoot apex of *Arabidopsis thaliana*. *Development* 131, 4225-4237.
- 600 24. Long, J., and Barton, M.K. (2000). Initiation of axillary and floral meristems in *Arabidopsis*.  
601 *Developmental biology* 218, 341-353.
- 602 25. Kayes, J.M., and Clark, S.E. (1998). CLAVATA2, a regulator of meristem and organ  
603 development in *Arabidopsis*. *Development* 125, 3843-3851.
- 604 26. Rédei, J. (1992). A note on Columbia wild type and Landsberg erecta. *Methods in  
605 Arabidopsis Research* 3.
- 606 27. Schultz, E.A., and Haughn, G.W. (1991). LEAFY, a homeotic gene that regulates  
607 inflorescence development in *Arabidopsis*. *The Plant Cell* 3, 771-781.
- 608 28. Clark, S.E., Williams, R.W., and Meyerowitz, E.M. (1997). The CLAVATA1 gene encodes  
609 a putative receptor kinase that controls shoot and floral meristem size in *Arabidopsis*. *Cell*  
610 89, 575-585.
- 611 29. DeYoung, B.J., Bickle, K.L., Schrage, K.J., Muskett, P., Patel, K., and Clark, S.E. (2006).  
612 The CLAVATA1-related BAM1, BAM2 and BAM3 receptor kinase-like proteins are  
613 required for meristem function in *Arabidopsis*. *The Plant Journal* 45, 1-16.
- 614 30. Nimchuk, Z.L., Zhou, Y., Tarr, P.T., Peterson, B.A., and Meyerowitz, E.M. (2015). Plant  
615 stem cell maintenance by transcriptional cross-regulation of related receptor kinases.  
616 *Development* 142, 1043-1049.

- 617 31. Hu, C., Zhu, Y., Cui, Y., Cheng, K., Liang, W., Wei, Z., Zhu, M., Yin, H., Zeng, L., and  
618 Xiao, Y. (2018). A group of receptor kinases are essential for CLAVATA signalling to  
619 maintain stem cell homeostasis. *Nature plants* 4, 205-211.
- 620 32. Song, S.-K., Lee, M.M., and Clark, S.E. (2006). POL and PLL1 phosphatases are  
621 CLAVATA1 signaling intermediates required for *Arabidopsis* shoot and floral stem cells.  
622 *Development* 133, 4691-4698.
- 623 33. Goad, D.M., Zhu, C., and Kellogg, E.A. (2017). Comprehensive identification and  
624 clustering of CLV3/ESR-related (CLE) genes in plants finds groups with potentially shared  
625 function. *New Phytologist* 216, 605-616.
- 626 34. Fletcher, J.C., Brand, U., Running, M.P., Simon, R., and Meyerowitz, E.M. (1999).  
627 Signaling of cell fate decisions by CLAVATA3 in *Arabidopsis* shoot meristems. *Science*  
628 283, 1911-1914.
- 629 35. Ogawa, M., Shinohara, H., Sakagami, Y., and Matsubayashi, Y. (2008). *Arabidopsis* CLV3  
630 peptide directly binds CLV1 ectodomain. *Science* 319, 294-294.
- 631 36. Lachowiec, J., Queitsch, C., and Kliebenstein, D.J. (2016). Molecular mechanisms  
632 governing differential robustness of development and environmental responses in plants.  
633 *Annals of botany* 117, 795-809.
- 634 37. Alonso-Blanco, C., El-Assal, S.E.-D., Coupland, G., and Koornneef, M. (1998). Analysis  
635 of natural allelic variation at flowering time loci in the Landsberg erecta and Cape Verde  
636 Islands ecotypes of *Arabidopsis thaliana*. *Genetics* 149, 749-764.
- 637 38. Gray, W.M., Östlin, A., Sandberg, G., Romano, C.P., and Estelle, M. (1998). High  
638 temperature promotes auxin-mediated hypocotyl elongation in *Arabidopsis*. *Proceedings*  
639 of the National Academy of Sciences 95, 7197-7202.
- 640 39. Quint, M., Delker, C., Franklin, K.A., Wigge, P.A., Halliday, K.J., and van Zanten, M.  
641 (2016). Molecular and genetic control of plant thermomorphogenesis. *Nature plants* 2, 1-  
642 9.

- 643 40. Franklin, K.A., Lee, S.H., Patel, D., Kumar, S.V., Spartz, A.K., Gu, C., Ye, S., Yu, P.,  
644 Breen, G., and Cohen, J.D. (2011). Phytochrome-interacting factor 4 (PIF4) regulates  
645 auxin biosynthesis at high temperature. *Proceedings of the National Academy of Sciences*  
646 108, 20231-20235.
- 647 41. Sun, J., Qi, L., Li, Y., Chu, J., and Li, C. (2012). PIF4-mediated activation of YUCCA8  
648 expression integrates temperature into the auxin pathway in regulating *Arabidopsis*  
649 hypocotyl growth. *PLoS genetics* 8.
- 650 42. Box, M.S., Huang, B.E., Domijan, M., Jaeger, K.E., Khattak, A.K., Yoo, S.J., Sedivy, E.L.,  
651 Jones, D.M., Hearn, T.J., and Webb, A.A. (2015). ELF3 controls thermoresponsive growth  
652 in *Arabidopsis*. *Current biology* 25, 194-199.
- 653 43. Ashburner, M., Ball, C.A., Blake, J.A., Botstein, D., Butler, H., Cherry, J.M., Davis, A.P.,  
654 Dolinski, K., Dwight, S.S., and Eppig, J.T. (2000). Gene ontology: tool for the unification  
655 of biology. *Nature genetics* 25, 25-29.
- 656 44. Consortium, G.O. (2019). The gene ontology resource: 20 years and still GOing strong.  
657 *Nucleic acids research* 47, D330-D338.
- 658 45. Mi, H., Muruganujan, A., Huang, X., Ebert, D., Mills, C., Guo, X., and Thomas, P.D. (2019).  
659 Protocol Update for large-scale genome and gene function analysis with the PANTHER  
660 classification system (v. 14.0). *Nature protocols* 14, 703-721.
- 661 46. Sabatini, S., Beis, D., Wolkenfelt, H., Murfett, J., Guilfoyle, T., Malamy, J., Benfey, P.,  
662 Leyser, O., Bechtold, N., and Weisbeek, P. (1999). An auxin-dependent distal organizer  
663 of pattern and polarity in the *Arabidopsis* root. *Cell* 99, 463-472.
- 664 47. Friml, J., Vieten, A., Sauer, M., Weijers, D., Schwarz, H., Hamann, T., Offringa, R., and  
665 Jürgens, G. (2003). Efflux-dependent auxin gradients establish the apical–basal axis of  
666 *Arabidopsis*. *Nature* 426, 147-153.

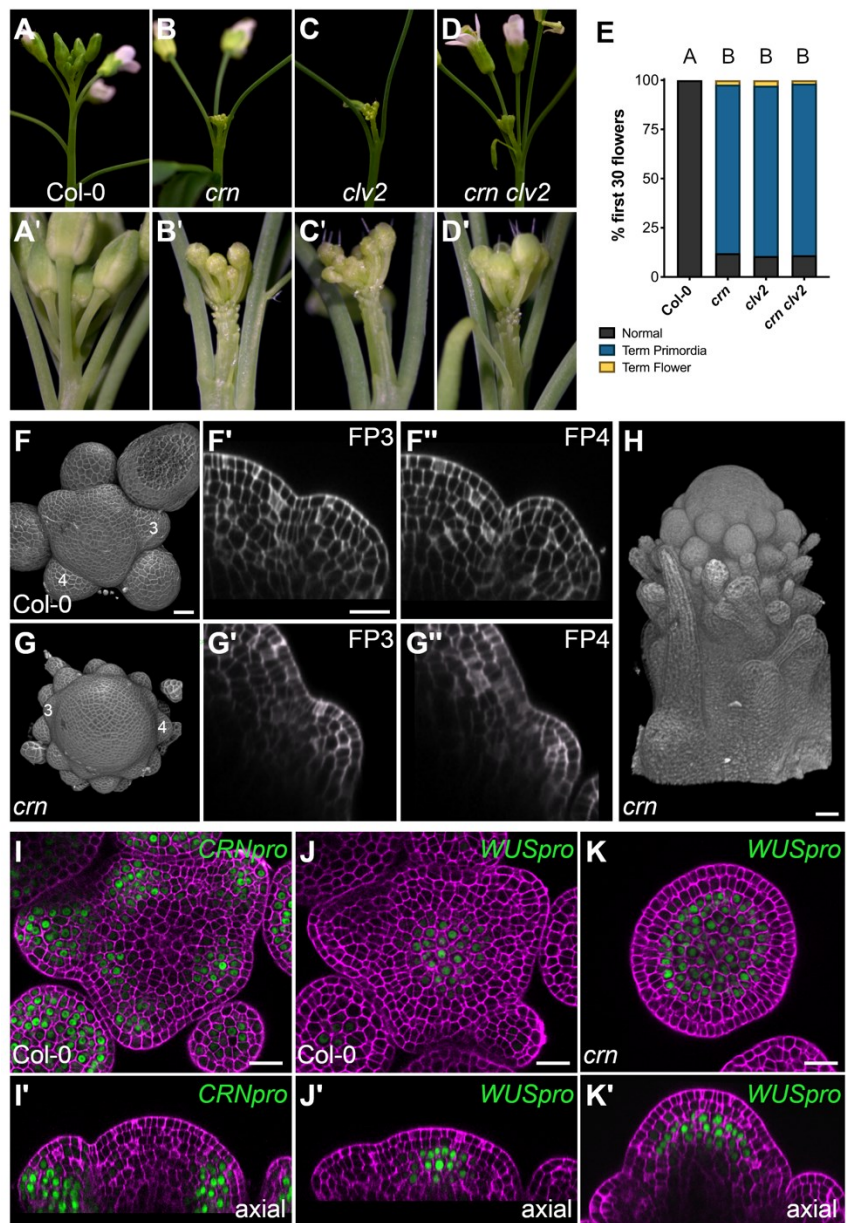
- 667 48. Cheng, Y., Dai, X., and Zhao, Y. (2006). Auxin biosynthesis by the YUCCA flavin  
668 monooxygenases controls the formation of floral organs and vascular tissues in  
669 *Arabidopsis*. *Genes & development* *20*, 1790-1799.
- 670 49. Krizek, B. (2009). AINTEGUMENTA and AINTEGUMENTA-LIKE6 act redundantly to  
671 regulate *Arabidopsis* floral growth and patterning. *Plant physiology* *150*, 1916-1929.
- 672 50. Prigge, M.J., Platret, M., Kadakia, N., Zhang, Y., Greenham, K., Szutu, W., Pandey, B.K.,  
673 Bhosale, R.A., Bennett, M.J., and Busch, W. (2020). Genetic analysis of the *Arabidopsis*  
674 TIR1/AFB auxin receptors reveals both overlapping and specialized functions. *Elife* *9*.
- 675 51. Mashiguchi, K., Tanaka, K., Sakai, T., Sugawara, S., Kawaide, H., Natsume, M., Hanada,  
676 A., Yaeno, T., Shirasu, K., and Yao, H. (2011). The main auxin biosynthesis pathway in  
677 *Arabidopsis*. *Proceedings of the National Academy of Sciences* *108*, 18512-18517.
- 678 52. Won, C., Shen, X., Mashiguchi, K., Zheng, Z., Dai, X., Cheng, Y., Kasahara, H., Kamiya,  
679 Y., Chory, J., and Zhao, Y. (2011). Conversion of tryptophan to indole-3-acetic acid by  
680 TRYPTOPHAN AMINOTRANSFERASES OF ARABIDOPSIS and YUCCAs in  
681 *Arabidopsis*. *Proceedings of the National Academy of Sciences* *108*, 18518-18523.
- 682 53. Lavy, M., and Estelle, M. (2016). Mechanisms of auxin signaling. *Development* *143*, 3226-  
683 3229.
- 684 54. Björkman, T., and Pearson, K.J. (1998). High temperature arrest of inflorescence  
685 development in broccoli (*Brassica oleracea* var. *italica* L.). *Journal of Experimental Botany*  
686 *49*, 101-106.
- 687 55. Anderson, R., Bayer, P.E., and Edwards, D. (2020). Climate change and the need for  
688 agricultural adaptation. *Current Opinion in Plant Biology*.
- 689 56. Torii, K.U., Mitsukawa, N., Oosumi, T., Matsuura, Y., Yokoyama, R., Whittier, R.F., and  
690 Komeda, Y. (1996). The *Arabidopsis* ERECTA gene encodes a putative receptor protein  
691 kinase with extracellular leucine-rich repeats. *The Plant Cell* *8*, 735-746.

- 692 57. Kinoshita, A., Betsuyaku, S., Osakabe, Y., Mizuno, S., Nagawa, S., Stahl, Y., Simon, R.,  
693 Yamaguchi-Shinozaki, K., Fukuda, H., and Sawa, S. (2010). RPK2 is an essential  
694 receptor-like kinase that transmits the CLV3 signal in *Arabidopsis*. *Development* 137,  
695 3911-3920.
- 696 58. Lita, P.Y., Miller, A.K., and Clark, S.E. (2003). POLTERGEIST encodes a protein  
697 phosphatase 2C that regulates CLAVATA pathways controlling stem cell identity at  
698 *Arabidopsis* shoot and flower meristems. *Current Biology* 13, 179-188.
- 699 59. Hicks, K.A., Millar, A.J., Carre, I.A., Somers, D.E., Straume, M., Meeks-Wagner, D.R., and  
700 Kay, S.A. (1996). Conditional circadian dysfunction of the *Arabidopsis* early-flowering 3  
701 mutant. *Science* 274, 790-792.
- 702 60. Hazak, O., Brandt, B., Cattaneo, P., Santiago, J., Rodriguez-Villalon, A., Hothorn, M., and  
703 Hardtke, C.S. (2017). Perception of root-active CLE peptides requires CORYNE function  
704 in the phloem vasculature. *EMBO reports* 18, 1367-1381.
- 705 61. Blilou, I., Xu, J., Wildwater, M., Willemse, V., Paponov, I., Friml, J., Heidstra, R., Aida,  
706 M., Palme, K., and Scheres, B. (2005). The PIN auxin efflux facilitator network controls  
707 growth and patterning in *Arabidopsis* roots. *Nature* 433, 39-44.
- 708 62. Zhang, W., To, J.P., Cheng, C.Y., Eric Schaller, G., and Kieber, J.J. (2011). Type-A  
709 response regulators are required for proper root apical meristem function through post-  
710 transcriptional regulation of PIN auxin efflux carriers. *The Plant Journal* 68, 1-10.
- 711 63. Vernoux, T., Brunoud, G., Farcot, E., Morin, V., Van den Daele, H., Legrand, J., Oliva, M.,  
712 Das, P., Larrieu, A., and Wells, D. (2011). The auxin signalling network translates dynamic  
713 input into robust patterning at the shoot apex. *Molecular systems biology* 7, 508.
- 714 64. Wiśniewska, J., Xu, J., Seifertová, D., Brewer, P.B., Růžička, K., Blilou, I., Rouquié, D.,  
715 Benková, E., Scheres, B., and Friml, J. (2006). Polar PIN localization directs auxin flow in  
716 plants. *Science* 312, 883-883.

- 717 65. Peterson, B.A., Haak, D.C., Nishimura, M.T., Teixeira, P.J., James, S.R., Dangl, J.L., and  
718 Nimchuk, Z.L. (2016). Genome-wide assessment of efficiency and specificity in  
719 CRISPR/Cas9 mediated multiple site targeting in *Arabidopsis*. *PLoS one* 11.
- 720 66. LeBlanc, C., Zhang, F., Mendez, J., Lozano, Y., Chatpar, K., Irish, V.F., and Jacob, Y.  
721 (2018). Increased efficiency of targeted mutagenesis by CRISPR/Cas9 in plants using  
722 heat stress. *The Plant Journal* 93, 377-386.
- 723 67. Hodgens, C., Nimchuk, Z.L., and Kieber, J.J. (2017). indCAPS: A tool for designing  
724 screening primers for CRISPR/Cas9 mutagenesis events. *PLoS one* 12.
- 725 68. Clough, S.J., and Bent, A.F. (1998). Floral dip: a simplified method for *Agrobacterium*-  
726 mediated transformation of *Arabidopsis thaliana*. *The plant journal* 16, 735-743.
- 727 69. Ishihara, H., Sugimoto, K., Tarr, P.T., Temman, H., Kadokura, S., Inui, Y., Sakamoto, T.,  
728 Sasaki, T., Aida, M., and Suzuki, T. (2019). Primed histone demethylation regulates shoot  
729 regenerative competency. *Nature communications* 10, 1-15.
- 730 70. Prunet, N., Jack, T.P., and Meyerowitz, E.M. (2016). Live confocal imaging of *Arabidopsis*  
731 flower buds. *Developmental biology* 419, 114-120.
- 732 71. Nimchuk, Z.L., and Perdue, T.D. (2017). Live imaging of shoot meristems on an inverted  
733 confocal microscope using an objective lens inverter attachment. *Frontiers in plant science*  
734 8, 773.
- 735 72. Schindelin, J., Arganda-Carreras, I., Frise, E., Kaynig, V., Longair, M., Pietzsch, T.,  
736 Preibisch, S., Rueden, C., Saalfeld, S., and Schmid, B. (2012). Fiji: an open-source  
737 platform for biological-image analysis. *Nature methods* 9, 676-682.
- 738 73. Pertea, M., Kim, D., Pertea, G.M., Leek, J.T., and Salzberg, S.L. (2016). Transcript-level  
739 expression analysis of RNA-seq experiments with HISAT, StringTie and Ballgown. *Nat  
740 Protoc* 11, 1650-1667.
- 741 74. Liao, Y., Smyth, G.K., and Shi, W. (2013). The Subread aligner: fast, accurate and  
742 scalable read mapping by seed-and-vote. *Nucleic acids research* 41, e108-e108.

- 743 75. Risso, D., Schwartz, K., Sherlock, G., and Dudoit, S. (2011). GC-Content Normalization  
744 for RNA-Seq Data. *BMC Bioinformatics* 12, 480.
- 745 76. Risso, D., Ngai, J., Speed, T.P., and Dudoit, S. (2014). Normalization of RNA-seq data  
746 using factor analysis of control genes or samples. *Nature biotechnology* 32, 896-902.
- 747 77. Robinson, M.D., McCarthy, D.J., and Smyth, G.K. (2010). edgeR: a Bioconductor package  
748 for differential expression analysis of digital gene expression data. *Bioinformatics* 26, 139-  
749 140.
- 750 78. Thomas, P.D., Campbell, M.J., Kejariwal, A., Mi, H., Karlak, B., Daverman, R., Diemer, K.,  
751 Muruganujan, A., and Narechania, A. (2003). PANTHER: A Library of Protein Families  
752 and Subfamilies Indexed by Function. *Genome Research* 13, 2129-2141.
- 753 79. Bray, N.L., Pimentel, H., Melsted, P., and Pachter, L. (2016). Near-optimal probabilistic  
754 RNA-seq quantification. *Nature Biotechnology* 34, 525-527.
- 755 80. Pimentel, H., Bray, N.L., Puente, S., Melsted, P., and Pachter, L. (2017). Differential  
756 analysis of RNA-seq incorporating quantification uncertainty. *Nature methods* 14, 687-  
757 690.
- 758
- 759

760 **Figure 1**

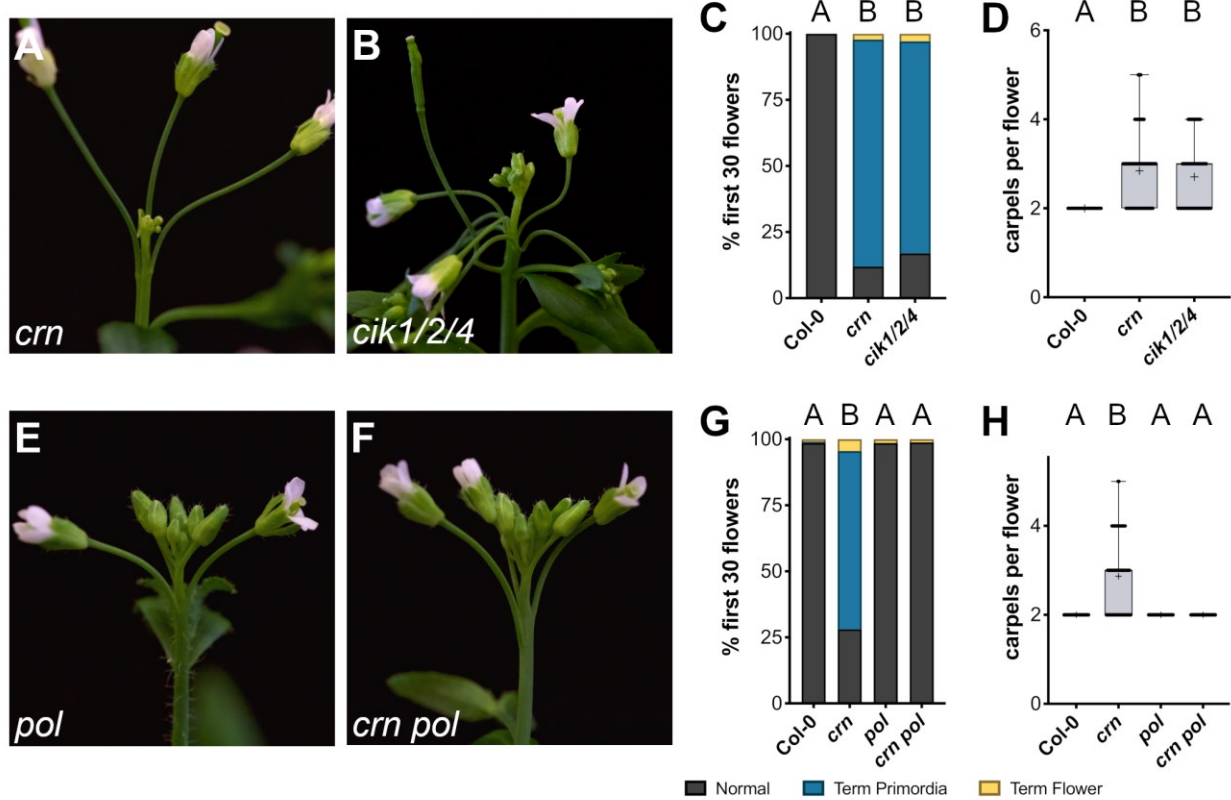


761

762

763 **Figure 2**

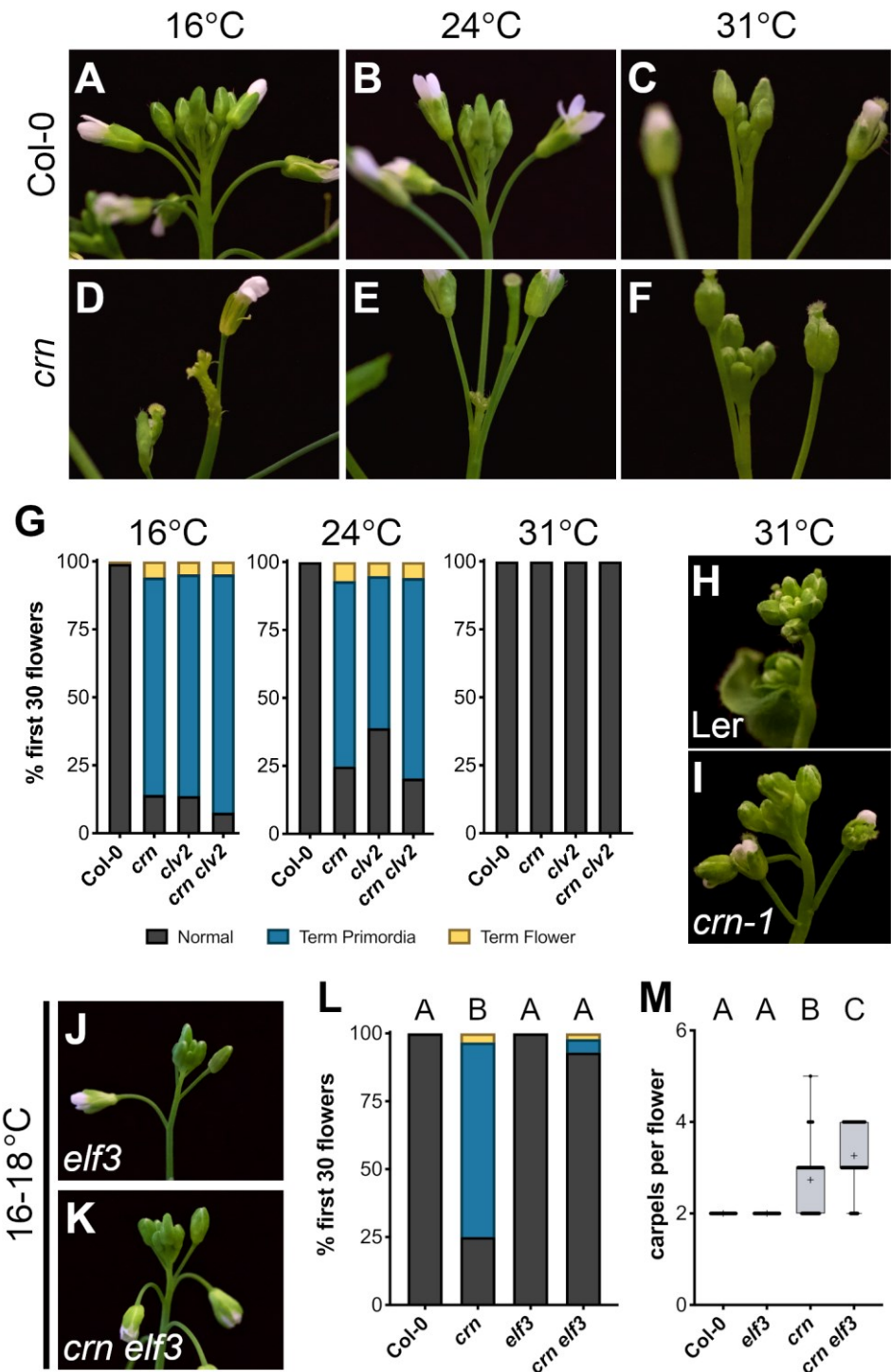
764



765

766

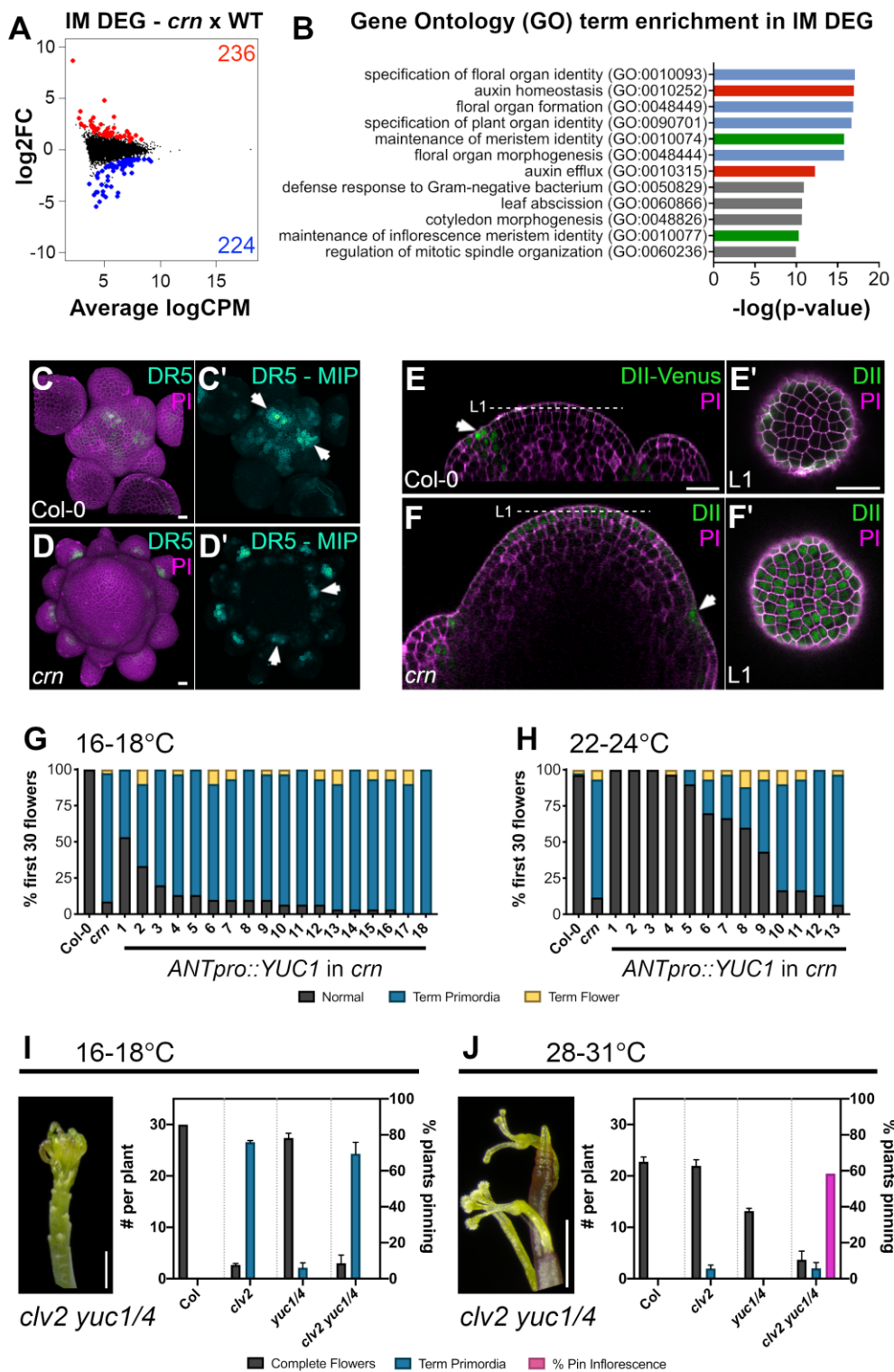
767 **Figure 3**



768

769

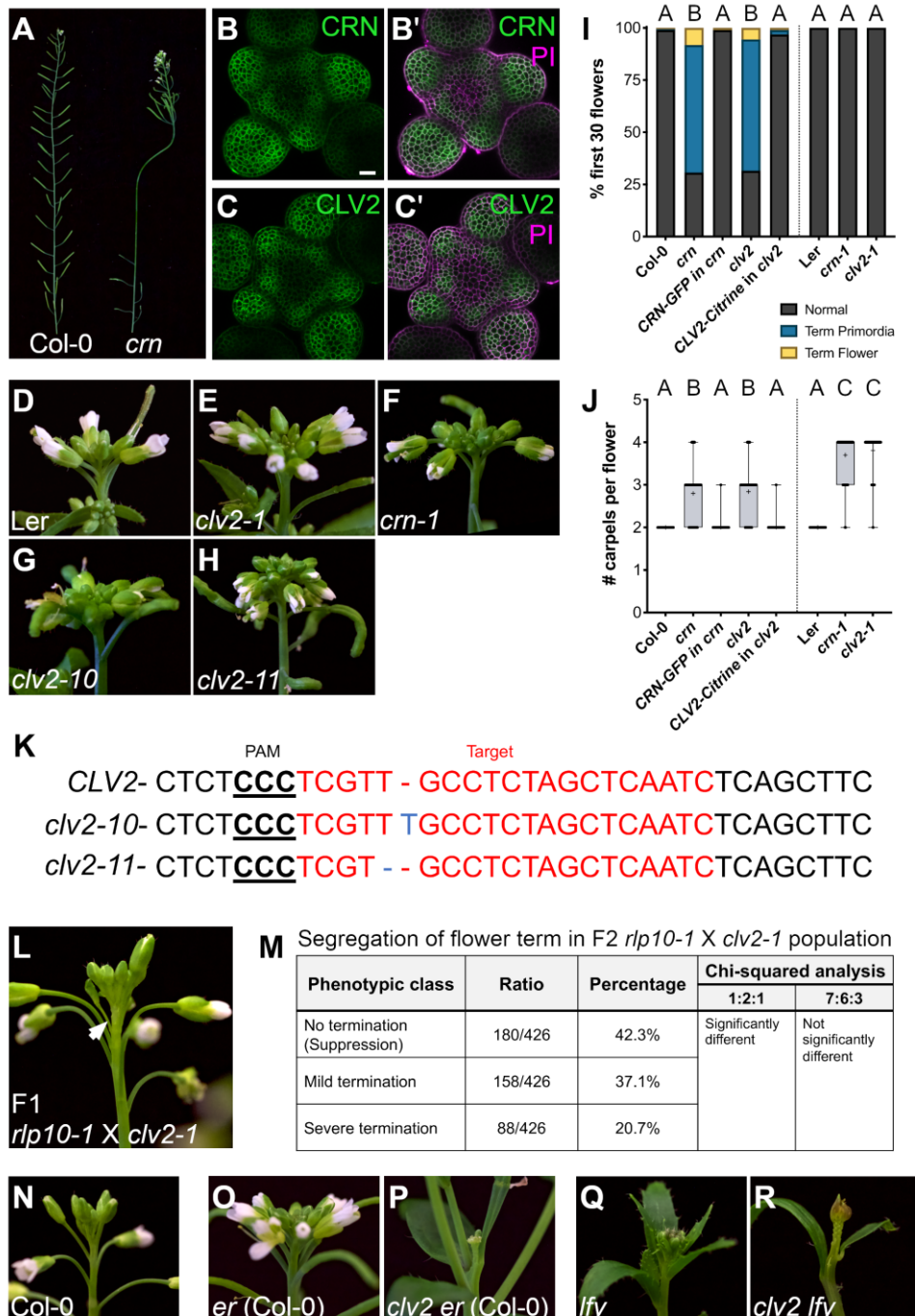
770 **Figure 4**



771

772

773 **Supplemental**

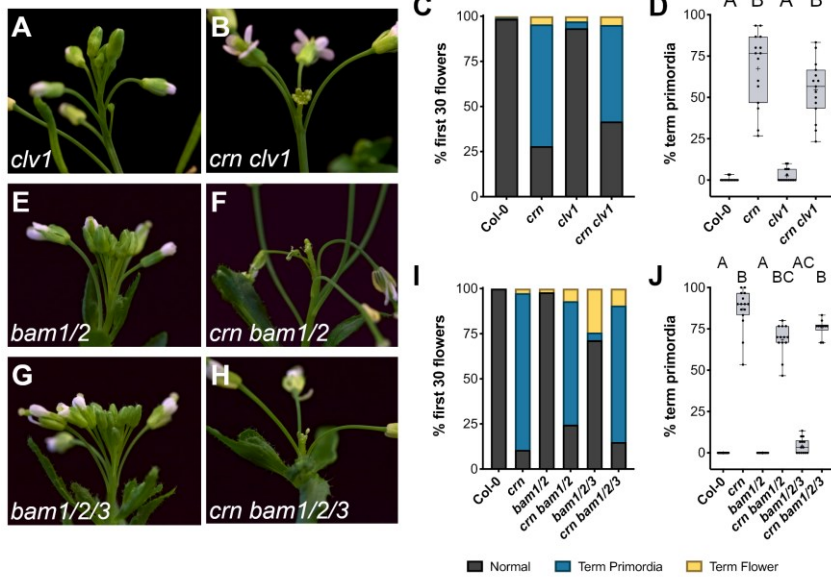


815 **Figure S1. CLV2/CRN regulate primordia outgrowth in an ecotype-dependent manner.**  
 816 **Related to Figure 1**

817 (A) Inflorescence architecture of *Col-0* and *crn*, showing bare stem (flower termination) and  
 818 recovery of *crn* compared to continuous flower production in *Col-0*. (B-C) *CRNpro::CRN-GFP* in

819 *crn* and *CLV2pro::CLV2-GFP* in *clv2* (*rlp10-1*) are expressed in developing flower primordia. PI  
820 (magenta) stained IM's of (B') *CRN-GFP* (green; n=6) and (C') *CLV2-Citrine* (green; n=5). (D-H)  
821 Inflorescences of *crn-1* and multiple *clv2* mutant alleles in the Ler background.(I-J) Quantification  
822 of (I) flower termination and (J) carpel number in Col-0 (n=16), *crn* (n=15), *CRNpro:CRN-GFP* in  
823 *crn* (n=16), *clv2* (*rlp10-1*) (n=15), *CLV2pro:CLV2-Citrine* in *clv2* (*rlp10-1*, n=16), Ler (n=18), *crn-1*  
824 (n=16) and *clv2-1* (n=14).(K) Novel CRISPR alleles of *clv2* in the Ler background. Target  
825 sequences are in red, edits (insertions and deletions) are shown in blue, and protospacer adjacent  
826 motif (PAM) is underlined. (L) Inflorescence of F1 hybrid from *clv2* (*rlp10-1* X *clv2-1*). Terminated  
827 primordia shown by arrow. (M) Segregation of flower termination defects in F2 mapping  
828 population of *rlp10-1* X *clv2-1*. (N-R) Inflorescences of (N) Col-0, (O) *erecta* (*er-105*), (P) *clv2 er*  
829 (in the Col-0 background), (Q) *leafy* (*Ify-1*), and (R) *clv2 Ify* (in the Col-0 background). Scale bars,  
830 20 $\mu$ m (B-C). Box and whisker plots show full range of data (min to max) with mean marked with  
831 "+" . Statistical groupings based on significant differences found using Kruskal-Wallis and Dunn's  
832 multiple comparison test correction, significance defined as p-value < 0.05 (I-J).  
833  
834  
835  
836  
837  
838  
839  
840  
841  
842  
843  
844  
845  
846  
847  
848  
849  
850  
851  
852  
853  
854  
855  
856  
857  
858  
859  
860  
861  
862  
863  
864

865  
866  
867  
868  
869  
870  
871  
872  
873  
874  
875  
876  
877  
878  
879  
880



881

882 *CIK1* WT- TCTCTTCTGCTACACT - TTCTCCTACTTGGTGTAA  
883 m - TCTCTTCTGCTACACTCTTCTGCTACTTGGTGTAA

884 *CIK2* WT- TTCCAGAGGAGCTCCAAGTCAGTCTCTTCAGG  
885 m - TTCCAGAG - - - GTCAGTCTCTTCAGG

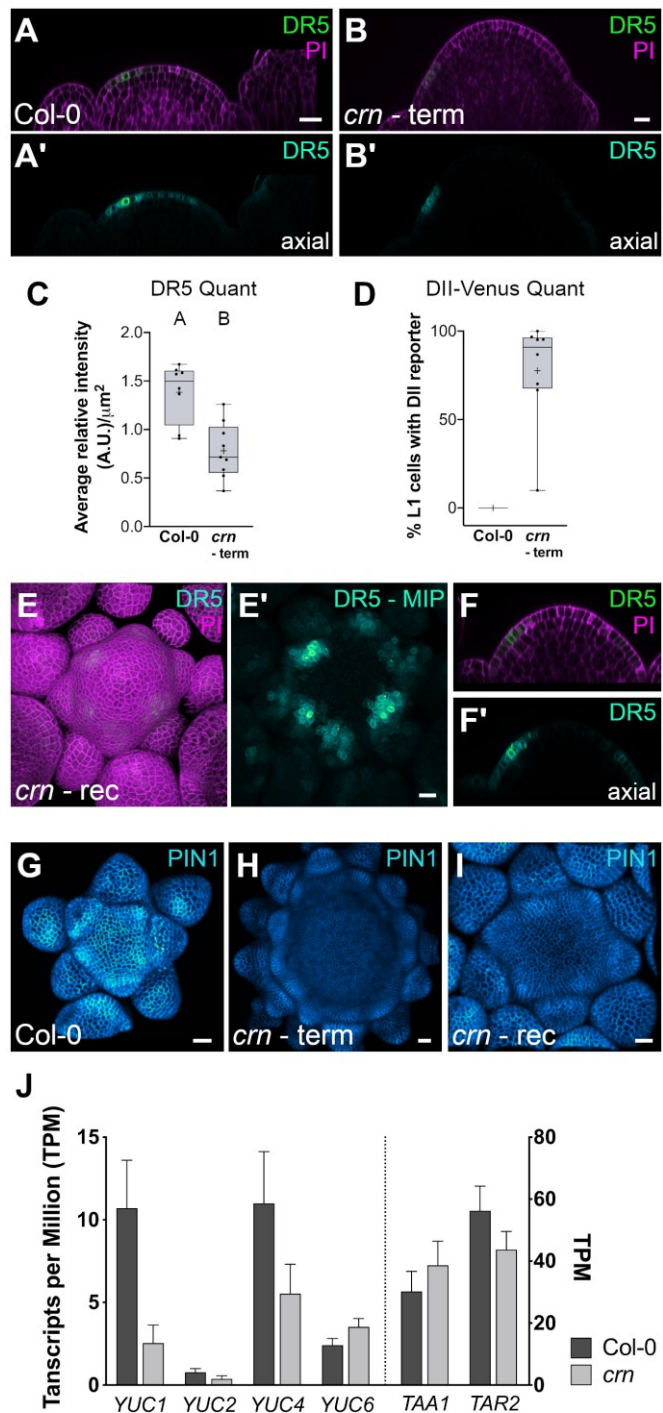
886 *CIK4* WT-TGAAAGATGAGAAAGAGGTTT - GTCTGGTTGG  
m - TGAAAGATGAGAAAGAGGTTTGTCTGGTTGG



887 **Figure S2. CLV2/CRN-mediated flower primordia outgrowth is independent of CLV1/BAM  
888 receptors and CLV3 peptide signaling. Related to Figure 2**

889 (A-D) Inflorescences of (A) *clv1* (*clv1-101*) and (B) *crn clv1*. (C-D) Quantification of (C) flower  
890 primordia termination and (D) comparisons of termination percentages in *Col-0* (n=15), *crn*  
891 (n=15), *clv1* (n=17), and *crn clv1* (n=15). (E-J) Inflorescences of (E) *bam1/2* (*bam1-4, bam2-4*),  
892 (F) *crn bam1/2*, (G) *bam1/2/3* (*bam1-4/bam2-4/bam3-2*) and (H) *crn bam1/2/3*. (I-J) Quantification  
893 of (I) flower primordia termination and (J) comparisons of primordia termination percentages in  
894 *Col-0* (n=16), *crn* (n=15), *bam1/2* (n=10), *crn bam1/2* (n=13), *bam1/2/3* (n=14), *crn bam1/2/3*  
895 (n=10). (K) Novel CRISPR alleles of *cik1/2/4* (*cik1-3/cik2-3/cik4-3*). Sequences of wildtype (WT)  
896 and edited (m) genomic DNA of *CIK1*, *CIK2*, and *CIK3*. Target sequences are in red, edits  
897 (insertions and deletions) are shown in blue, and protospacer adjacent motif (PAM) is underlined.  
898 (L-N) Inflorescences of (L) *clv3* (*clv3-9*), (M) *dodeca-cle* (*clv3-9, cle9, cle10, cle11, cle12, cle13,*  
899 *cle18, cle19, cle20, cle21, cle22, cle45*) and (N) *crn clv3*. Box and whisker plots show full range  
900 of data (min to max) with mean marked with "+". Statistical groupings based on significant  
901 differences found using Kruskal-Wallis and Dunn's multiple comparison test correction,  
902 significance defined as p-value < 0.05 (D and J).

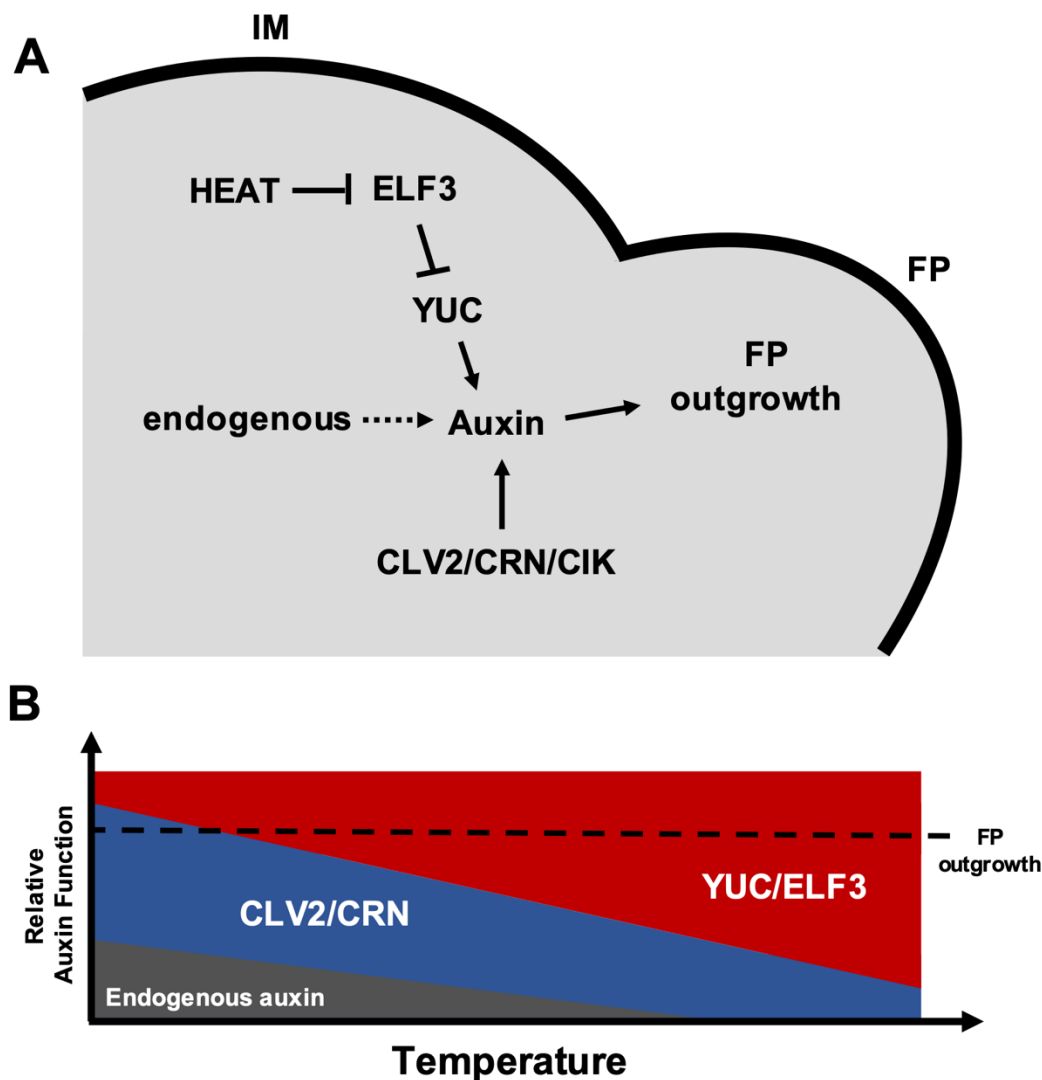
911  
912  
913  
914  
915  
916  
917  
918



950 **Figure S3. Auxin signaling is reduced in the *crn* inflorescence meristem during the**  
951 **termination phase. Related to Figure 4**

952 (A) Axial view of Col-0 inflorescence meristem showing L1 expression of (A) *DR5::GFP* (green)  
953 co-labeled with PI (magenta) and (A') a heatmap of the *DR5::GFP* (teal) signal on its own. Section  
954 corresponds to the developing primordia that had the highest DR5 levels. (B) Axial view of *crn*  
955 inflorescence meristem with L1 expression of (B) *DR5::GFP* (green) co-labeled with PI (magenta)

956 and (B') a heatmap of the *DR5::GFP* (teal) signal on its own. Section corresponds to the  
957 developing primordia that had the highest DR5 levels. (C) Quantification of *DR5::GFP* levels in  
958 Col-0 (n=8) compared to terminated *crn* (n=9) IMs. (D) Quantification of *DII-Venus* in Col-0 (n=4)  
959 compared to terminated *crn* (n=8) IMs, using percentage of L1 layer cells with reporter for  
960 comparison. (E) Maximum intensity projection (MIP) of *DR5::GFP* (teal) in the inflorescence  
961 meristem of *crn* after floral recovery (n=4). Tissue stained with PI (magenta). (F) Axial view of  
962 recovered *crn* inflorescence meristem (*crn* - rec) with L1 expression of (F) *DR5::GFP* (green) co-  
963 labeled with PI (magenta) and (F') a heatmap of the *DR5::GFP* (teal) signal on its own. Section  
964 corresponds to the developing primordia that had the highest DR5 levels. (G-I) Maximum intensity  
965 projection (MIP) of *PIN1pro::PIN1-GFP* (blue heatmap) in the inflorescence meristem of: (G) Col-  
966 0 (n=16), (H) *crn* during termination (*crn* - term; n=19), (I) *crn* after floral recovery (*crn* - rec; n=5).  
967 (J) Expression levels of key auxin biosynthesis genes in Col-0 and *crn* IMs from RNAseq analysis.  
968 Genes included are *YUCCA* (*YUC*) 1/2/4/6, *TRYPTOPHAN AMINOTRANSFERASE OF*  
969 *ARABIDOPSIS* (*TAA1*), and *TRYPTOPHAN AMINOTRANSFERASE RELATED 2* (*TAR2*).  
970 *YUC1/2/4/6* levels shown on left y-axis; *TAA1* and *TAR2* levels are shown on right y-axis. Box  
971 and whisker plots show full range of data (min to max) with mean marked with “+”. Statistical  
972 grouping based on unpaired t-test with a p-value = 0.0007. Error bars = standard deviation. Scale  
973 bars, 20 $\mu$ m.  
974  
975  
976  
977  
978  
979  
980  
981  
982  
983  
984  
985  
986  
987  
988  
989  
990  
991  
992  
993  
994  
995  
996  
997  
998  
999  
1000  
1001



1002  
 1003  
 1004  
**Figure S4. Model of flower primordia outgrowth. Related to Figures 1, 3, and 4**  
 1005  
 1006  
 1007  
 1008  
 1009  
 1010  
 1011  
 1012  
 1013  
 1014

GO Term Analysis								
GO Term	GO biological process	Annotation	Significant	Expected	over/under	fold Enrichment	P-value	FDR
GO:0010093	specification of floral organ identity	13	5	0.21	+	23.8	7.18E-06	9.14E-04
GO:0060866	leaf abscission	8	3	0.13	+	23.21	5.99E-04	3.26E-02
GO:0090701	specification of plant organ identity	14	5	0.23	+	22.1	9.62E-06	1.13E-03
GO:0010077	maintenance of inflorescence meristem identity	9	3	0.15	+	20.63	7.90E-04	4.00E-02
GO:0060236	regulation of mitotic spindle organization	10	3	0.16	+	18.57	1.01E-03	4.67E-02
GO:0060237	regulation of spindle organization	10	3	0.16	+	18.57	1.01E-03	4.63E-02
GO:0090224	auxin efflux	15	4	0.24	+	16.5	2.02E-04	1.41E-02
GO:0048449	floral organ formation	25	6	0.4	+	14.85	8.21E-06	9.83E-04
GO:0050829	defense response to Gram-negative bacterium	20	4	0.32	+	12.38	5.21E-04	2.94E-02
GO:0048826	cotyledon morphogenesis	21	4	0.34	+	11.79	6.12E-04	3.30E-02
GO:0010252	auxin homeostasis	39	7	0.63	+	11.11	7.68E-06	9.58E-04
GO:0010074	maintenance of meristem identity	45	7	0.73	+	9.63	1.77E-05	1.86E-03
GO:0048444	floral organ morphogenesis	45	7	0.73	+	9.63	1.77E-05	1.83E-03
GO:0006342	chromatin silencing	35	5	0.57	+	8.84	4.14E-04	2.43E-02
GO:0019827	stem cell population maintenance	55	7	0.89	+	7.88	5.67E-05	4.65E-03
GO:0010374	stomatal complex development	55	7	0.89	+	7.88	5.67E-05	4.59E-03
GO:0098727	maintenance of cell number	55	7	0.89	+	7.88	5.67E-05	4.53E-03
GO:0045814	negative regulation of gene expression, epigenetic	41	5	0.66	+	7.55	7.97E-04	4.01E-02
GO:0010928	regulation of auxin mediated signaling pathway	42	5	0.68	+	7.37	8.80E-04	4.15E-02
GO:0048481	plant ovule development	53	6	0.86	+	7.01	3.45E-04	2.13E-02
GO:0009914	hormone transport	90	10	1.45	+	6.88	4.52E-06	6.14E-04
GO:0035670	plant-type ovary development	55	6	0.89	+	6.75	4.15E-04	2.41E-02
GO:0048825	cotyledon development	55	6	0.89	+	6.75	4.15E-04	2.38E-02
GO:0060918	auxin transport	87	9	1.41	+	6.4	2.29E-05	2.21E-03
GO:0009926	auxin polar transport	69	7	1.11	+	6.28	2.08E-04	1.40E-02
GO:0009665	leaf morphogenesis	93	9	1.5	+	5.99	3.72E-05	3.32E-03
GO:0090698	post-embryonic plant morphogenesis	198	19	3.2	+	5.94	2.31E-09	1.15E-06
GO:0048440	carpel development	76	7	1.23	+	5.7	3.60E-04	2.20E-02
GO:0010016	shoot system morphogenesis	170	15	2.75	+	5.46	3.08E-07	8.00E-05
GO:0009908	flower development	354	30	5.72	+	5.24	9.63E-13	1.44E-09
GO:0090567	reproductive shoot system development	369	31	5.96	+	5.2	4.93E-13	9.83E-10
GO:0003002	regionalization	155	13	2.5	+	5.19	3.18E-06	5.14E-04
GO:0048467	gynoecium development	89	7	1.44	+	4.87	8.66E-04	4.15E-02
GO:0048437	floral organ development	243	19	3.93	+	4.84	4.96E-08	1.41E-05
GO:0006928	movement of cell or subcellular component	91	7	1.47	+	4.76	9.79E-04	4.54E-02
GO:0010073	meristem maintenance	145	11	2.34	+	4.69	4.29E-05	3.72E-03
GO:0007388	pattern specification process	188	14	3.04	+	4.61	4.87E-06	6.48E-04
GO:0048438	floral whorl development	193	14	3.12	+	4.49	6.46E-06	8.40E-04
GO:1905393	plant organ formation	111	8	1.79	+	4.46	6.47E-04	3.37E-02
GO:0009909	regulation of flower development	167	12	2.7	+	4.45	3.20E-05	2.90E-03
GO:0090697	post-embryonic plant organ morphogenesis	117	8	1.89	+	4.23	8.94E-04	4.18E-02
GO:0048367	shoot system development	724	49	11.7	+	4.19	2.04E-16	1.22E-12
GO:0048507	meristem development	217	14	3.51	+	3.99	2.23E-05	2.19E-03
GO:0048646	anatomical structure formation involved in morphogenesis	204	13	3.3	+	3.94	4.90E-05	4.19E-03
GO:0048831	regulation of shoot system development	268	17	4.33	+	3.93	3.73E-06	5.44E-04
GO:0048827	phyllome development	492	31	7.95	+	3.9	4.46E-10	2.96E-07
GO:001666	response to hypoxia	261	16	4.22	+	3.79	1.07E-05	1.23E-03
GO:0045944	positive regulation of transcription by RNA polymerase II	214	13	3.46	+	3.76	7.76E-05	6.03E-03
GO:0036293	response to decreased oxygen levels	265	16	4.28	+	3.74	1.28E-05	1.42E-03
GO:0070482	response to oxygen levels	266	16	4.3	+	3.72	1.34E-05	1.46E-03
GO:0046777	protein autophosphorylation	188	11	3.04	+	3.62	3.68E-04	2.18E-02
GO:0048366	leaf development	332	19	5.36	+	3.54	4.19E-06	5.83E-04
GO:0090696	post-embryonic plant organ development	176	10	2.84	+	3.52	8.34E-04	4.12E-02
GO:0010817	regulation of hormone levels	249	14	4.02	+	3.48	9.11E-05	6.99E-03
GO:0071456	cellular response to hypoxia	235	13	3.8	+	3.42	1.87E-04	1.33E-02
GO:0071453	cellular response to oxygen levels	237	13	3.83	+	3.39	2.03E-04	1.39E-02
GO:0036294	cellular response to decreased oxygen levels	237	13	3.83	+	3.39	2.03E-04	1.38E-02
GO:0009888	tissue development	605	31	9.78	+	3.17	4.35E-08	1.30E-05
GO:1905392	plant organ morphogenesis	403	20	6.51	+	3.07	1.73E-05	1.85E-03
GO:0014070	response to organic cyclic compound	287	14	4.64	+	3.02	3.66E-04	2.19E-02
GO:0009733	response to auxin	299	14	4.83	+	2.9	5.40E-04	2.99E-02
GO:0009653	anatomical structure morphogenesis	886	41	14.32	+	2.86	4.47E-09	1.91E-06
GO:0099402	plant organ development	996	44	16.09	+	2.73	4.48E-09	1.79E-06
GO:0048580	regulation of post-embryonic development	395	17	6.38	+	2.66	3.65E-04	2.21E-02
GO:2000241	regulation of reproductive process	374	16	6.04	+	2.65	5.73E-04	3.15E-02
GO:0006357	regulation of transcription by RNA polymerase II	430	18	6.95	+	2.59	3.41E-04	2.12E-02
GO:1902680	positive regulation of RNA biosynthetic process	521	21	8.42	+	2.49	1.84E-04	1.35E-02
GO:1903508	positive regulation of nucleic acid-templated transcription	521	21	8.42	+	2.49	1.84E-04	1.33E-02
GO:0048600	reproductive structure development	1198	48	19.36	+	2.48	1.79E-08	6.69E-06
GO:0061458	reproductive system development	1200	48	19.39	+	2.48	1.87E-08	6.58E-06
GO:2000026	regulation of multicellular organismal development	568	22	9.18	+	2.4	2.94E-04	1.91E-02
GO:0010557	positive regulation of macromolecule biosynthetic process	569	22	9.19	+	2.39	2.98E-04	1.89E-02
GO:0045898	positive regulation of transcription, DNA-templated	519	20	8.39	+	2.38	6.15E-04	3.29E-02
GO:0042592	homeostatic process	522	20	8.43	+	2.37	6.40E-04	3.39E-02
GO:0051254	positive regulation of RNA metabolic process	550	21	8.89	+	2.36	4.66E-04	2.65E-02
GO:0031328	positive regulation of cellular biosynthetic process	603	23	9.74	+	2.36	2.39E-04	1.59E-02
GO:0009891	positive regulation of biosynthetic process	620	23	10.02	+	2.3	3.22E-04	2.03E-02
GO:0045935	positive regulation of nucleobase-containing compound metabolic	570	21	9.21	+	2.28	6.46E-04	3.39E-02
GO:0009791	post-embryonic development	1472	54	23.79	+	2.27	3.87E-08	1.22E-05
GO:0051173	positive regulation of nitrogen compound metabolic process	739	27	11.94	+	2.26	1.67E-04	1.23E-02
GO:0048731	system development	1849	67	29.88	+	2.24	1.09E-09	5.92E-07
GO:0003004	developmental process involved in reproduction	1427	51	23.06	+	2.21	2.66E-07	7.25E-05
GO:0051239	regulation of multicellular organismal process	625	22	10.1	+	2.18	1.09E-03	4.88E-02
GO:0050793	regulation of developmental process	781	27	12.62	+	2.14	2.94E-04	1.89E-02
GO:0031325	positive regulation of cellular metabolic process	797	27	12.88	+	2.1	5.23E-04	2.93E-02
GO:0010604	positive regulation of macromolecule metabolic process	771	26	12.46	+	2.09	7.31E-04	3.74E-02
GO:0065004	regulation of biological quality	955	32	15.43	+	2.07	1.42E-04	1.08E-02
GO:0009725	response to hormone	1237	41	19.99	+	2.05	2.66E-05	2.45E-03
GO:0009719	response to endogenous stimulus	1274	42	20.59	+	2.04	2.12E-05	2.15E-03
GO:0048856	anatomical structure development	2824	93	45.63	+	2.04	6.09E-11	5.21E-08
GO:0007275	multicellular organism development	2436	80	39.36	+	2.03	2.53E-09	1.16E-06

GO Term	GO biological process	Annotation	Significant	Expected	over/under	fold Enrichment	P-value	FDR
GO:0006468	protein phosphorylation	1037	34	16.76	+	2.03	1.45E-04	1.09E-02
GO:0048522	positive regulation of cellular process	1055	34	17.05	+	1.99	2.67E-04	1.75E-02
GO:0070887	cellular response to chemical stimulus	1088	35	17.58	+	1.99	2.01E-04	1.41E-02
GO:0010033	response to organic substance	1711	55	27.65	+	1.99	1.77E-06	3.91E-04
GO:0022414	reproductive process	1714	55	27.7	+	1.99	1.83E-06	3.79E-04
GO:0000003	reproduction	1724	55	27.86	+	1.97	2.86E-06	5.04E-04
GO:0032502	developmental process	2979	93	48.14	+	1.93	8.62E-10	5.16E-07
GO:0009605	response to external stimulus	1508	47	24.37	+	1.93	2.42E-05	2.30E-03
GO:1901700	response to oxygen-containing compound	1511	47	24.42	+	1.93	2.50E-05	2.34E-03
GO:0032501	multicellular organismal process	2711	83	43.81	+	1.89	2.37E-08	7.89E-06
GO:0043207	response to external biotic stimulus	1092	33	17.65	+	1.87	8.62E-04	4.20E-02
GO:0051707	response to other organism	1092	33	17.65	+	1.87	8.62E-04	4.16E-02
GO:0009607	response to biotic stimulus	1093	33	17.66	+	1.87	8.68E-04	4.12E-02
GO:0006355	regulation of transcription, DNA-templated	2158	64	34.87	+	1.84	3.42E-06	5.38E-04
GO:1903506	regulation of nucleic acid-templated transcription	2158	64	34.87	+	1.84	3.42E-06	5.24E-04
GO:2001141	regulation of RNA biosynthetic process	2160	64	34.9	+	1.83	3.48E-06	5.21E-04
GO:0016310	phosphorylation	1216	36	19.65	+	1.83	6.87E-04	3.55E-02
GO:2000112	regulation of cellular macromolecule biosynthetic process	2340	69	37.81	+	1.82	2.08E-06	4.02E-04
GO:0044419	interspecies interaction between organisms	1120	33	18.1	+	1.82	1.09E-03	4.94E-02
GO:0010556	regulation of macromolecule biosynthetic process	2353	69	38.02	+	1.81	2.22E-06	4.16E-04
GO:0019219	regulation of nucleobase-containing compound metabolic process	2320	68	37.49	+	1.81	2.92E-06	4.85E-04
GO:0031326	regulation of cellular biosynthetic process	2451	71	39.6	+	1.79	2.28E-06	4.13E-04
GO:0009889	regulation of biosynthetic process	2488	72	40.2	+	1.79	1.81E-06	3.88E-04
GO:0051252	regulation of RNA metabolic process	2260	65	36.52	+	1.78	8.13E-06	9.93E-04
GO:0007165	signal transduction	1330	38	21.49	+	1.77	8.22E-04	4.10E-02
GO:0031323	regulation of cellular metabolic process	2956	84	47.76	+	1.76	4.50E-07	1.08E-04
GO:0060255	regulation of macromolecule metabolic process	3030	86	48.96	+	1.76	3.95E-07	9.86E-05
GO:0050794	regulation of cellular process	4726	134	76.36	+	1.75	2.97E-11	2.96E-08
GO:0051171	regulation of nitrogen compound metabolic process	2722	77	43.98	+	1.75	2.02E-06	4.03E-04
GO:0042221	response to chemical	2682	75	43.34	+	1.73	3.92E-06	5.59E-04
GO:0065007	biological regulation	5956	166	96.24	+	1.72	9.50E-14	2.84E-10
GO:0080090	regulation of primary metabolic process	2806	78	45.34	+	1.72	2.87E-06	4.91E-04
GO:0010468	regulation of gene expression	2648	73	42.79	+	1.71	1.09E-05	1.23E-03
GO:0019222	regulation of metabolic process	3302	91	53.36	+	1.71	4.96E-07	1.14E-04
GO:0050789	regulation of biological process	5374	148	86.84	+	1.7	1.46E-11	1.75E-08
GO:0051716	cellular response to stimulus	2521	69	40.74	+	1.69	2.20E-05	2.19E-03
GO:0007154	cell communication	1618	44	26.14	+	1.68	1.09E-03	4.91E-02
GO:0050896	response to stimulus	5567	149	89.95	+	1.66	9.48E-11	7.09E-08
GO:0006950	response to stress	3090	79	49.93	+	1.58	5.67E-05	4.71E-03
GO:0009987	cellular process	11959	237	193.24	+	1.23	3.89E-05	3.42E-03
GO:0016070	RNA metabolic process	1293	7	20.89	-	0.34	8.59E-04	4.21E-02
GO:0010467	gene expression	1601	8	25.87	-	0.31	5.35E-05	4.51E-03
GO:0006396	RNA processing	785	1	12.68	-	0.08	6.77E-05	5.33E-03

1016

1017

**Table S2. Full Gene Ontology terms list of top 460 DEGs in *crn* IMs. Related to Figure 4**

1019 The number of significant genes in our DEG list (p-value < 0.001) out of the annotated *A. thaliana*  
 1020 reference list from GO panther was used to calculate fold-enrichment, p-value and FDR. Red,  
 1021 green and blue highlighted GO processes indicate auxin, meristem and floral related genes,  
 1022 respectively, detailed further in Table S1.

1023

1024

1025

1026

1027

1028

1029

1030

1031

1032

1033

1034

1035

1036

1037

1038

1039

Auxin Biosynthetic Genes TPM Count						
	Gene Name	ATG - isoform	Col-0 TPM	crn TPM	p-value	q-value
1040	YUC1	AT4G32540.1	9.62163605	2.22777304	0.000150561	0.011150848
1041	YUC1	AT4G32540.2	1.08021526	0.30754248	0.066447724	0.246747862
1042	YUC2	AT4G13260.1	0.77819885	0.3726434	0.12364161	0.313064639
1043	YUC3	AT1G04610.1	0.05658348	0.05274052	0.542276947	0.648222557
1044	YUC4	AT5G11320.1	9.47973542	4.69456935	0.00471094	0.062519474
1045	YUC4	AT5G11320.2	1.51754126	0.83461118	0.044222831	0.204729205
1046	YUC5	AT5G43890.1	0.00390573	0	-	-
1047	YUC6	AT5G25620.1	2.41963745	3.5137845	0.054387715	0.226726537
1048	YUC7	AT2G33230.1	0.0058149	0	-	-
1049	YUC8	AT4G28720.1	0.07420622	0.02084606	-	-
1050	YUC9	AT1G04180.1	0.01755266	0.00867234	-	-
1051	YUC10	AT1G48910.1	0.01773398	0	-	-
1052	YUC11	AT1G21430.1	0	0	-	-
1053	TAA1	AT1G70560.1	30.226102	38.6519243	0.213430557	0.388882748
1054	TAR2	AT4G24670.1	9.30982625	5.82646658	0.065158626	0.244976736
1055	TAR2	AT4G24670.2	46.8980927	37.8726915	0.020707299	0.14162109
1056	AMI1	AT1G08980.1	38.6695782	61.3469622	0.00102772	0.027829535
1057	RHM3	AT3G14790.1	32.7962069	25.4270094	0.000729834	0.023526653
1058	ASB1	AT1G25220.1	36.6762453	34.5094303	0.096033747	0.286370868
1059	ASB1	AT1G25220.2	0.02064712	0.05240687	-	-
1060	VAS1	AT1G80360.1	20.8728462	13.2519822	0.006027497	0.07158872
1061	VAS1	AT1G80360.2	9.6028417	4.83430674	0.008223945	0.085497555
1062	VAS1	AT1G80360.3	2.59071657	2.7720062	0.388299567	0.529284096
1063	VAS1	AT1G80360.4	10.1510957	9.71721332	0.566011827	0.666634099
1064	AAO1	AT5G20960.1	0.85296647	0.92154705	1	1
1065	AAO1	AT5G20960.2	3.28165823	2.49653366	0.181870638	0.363877752

**Table S3. Average TPM and statistics of auxin biosynthetic genes in Col-0 and crn IMs. Related to Figure 4**

Grey boxes show *YUCCA* biosynthetic genes, light grey boxes show *TAA* family genes and white for other auxin biosynthetic genes.